

1 **Trehalose 6-phosphate regulates photosynthesis and assimilate partitioning in**  
2 **reproductive tissue**

3

4 Maria Oszvald, Lucia F. Primavesi, Cara A. Griffiths, Jonathan Cohn, Shib Sankar  
5 Basu, Michael L. Nuccio, and Matthew J. Paul<sup>1\*</sup>

6

7 Plant Science, Rothamsted Research, Harpenden, Hertfordshire, AL5 2JQ, United  
8 Kingdom (M.O., L.F.P., C.A.G., M.J.P.); Syngenta Crop Protection LLC, 9 Davis  
9 Drive, P.O. Box 12257, Research Triangle Park, North Carolina 27709, USA (J.C.,  
10 S.S.B., M.L.N.); Current address: Symmetry Bioanalytics, 104 TW Alexander Drive,  
11 Building 4, Research Triangle Park, NC 27709, USA (S.S.B.); Inari Agriculture, Inc.,  
12 200 Sidney Street St. 340, Cambridge MA 02139, USA (M.L.N.)

13 \*Correspondence: Matthew Paul ([matthew.paul@rothamsted.ac.uk](mailto:matthew.paul@rothamsted.ac.uk))

14 **Short title:** T6P regulates maize resource allocation

15 **One sentence summary:** Decreased T6P in phloem cells of maize female  
16 reproductive tissue causes opposing changes in primary and secondary metabolism  
17 and a shift in assimilates within cobs in favour of florets, simultaneously increasing  
18 photosynthetic rate.

19 **Author contributions:** SSB, MLN and MJP directed and designed the research.  
20 MO, LFP and CAG performed experiments. JC analyzed data. JC, MLN, SSB and  
21 MJP wrote the paper, which all authors edited and approved.

22 **Funding:** The work was funded by Syngenta. MJP acknowledges support from the  
23 Designing Future Wheat Institute Strategic Programme (BB/P016855/1).

24

25

26 **ABSTRACT**

27 Transgenic maize (*Zea mays*) that expresses rice (*Oryza sativa*) *TREHALOSE*  
28 *PHOSPHATE PHOSPHATASE1 (TPP1)* from the rice *MADS6* promoter, which is  
29 active over the flowering period, produces higher yields than wild type. This yield  
30 increase occurs with or without drought conditions during flowering. To understand  
31 the mechanistic basis of the increased yield, we characterised gene expression and  
32 metabolite profiles in leaves and developing female reproductive tissue – comprising  
33 florets, node, pith and shank – over the flowering period with and without drought.  
34 The *MADS6* promoter was most active in the vasculature, particularly phloem  
35 companion cells in florets and pith, consistent with the largest decreases in trehalose  
36 6-phosphate (T6P) levels (two- to threefold) being found in pith and florets. Low T6P  
37 led to decreased gene expression for primary metabolism and increased gene  
38 expression for secondary metabolism, particularly lipid-related pathways. Despite  
39 similar changes in gene expression, the pith and floret displayed opposing assimilate  
40 profiles: sugars, sugar phosphates, amino acids and lipids increased in florets, but  
41 decreased in pith. Possibly explaining this assimilate distribution, seven *SWEET*  
42 genes were found to be upregulated in the transgenic plants. SnRK1 activity and the,  
43 expression of the gene for the SnRK1 beta subunit, expression of SnRK1 marker  
44 genes, and endogenous trehalose pathway genes were also altered. Furthermore,  
45 leaves of the transgenic maize maintained a higher photosynthetic rate for a longer  
46 period compared to wild type. In conclusion, we found that decreasing T6P in  
47 reproductive tissues downregulates primary metabolism and upregulates secondary  
48 metabolism, resulting in different metabolite profiles in component tissues. Our data  
49 implicate T6P/ SnRK1 as a major regulator of whole-plant resource allocation for  
50 crop yield improvement.

51

52 **Key words:** Trehalose 6-phosphate, maize, SnRK1, sucrose, photosynthesis, crop  
53 yields, drought

54

55

56

57

58

59

## 60 INTRODUCTION

61 To avoid future food shortfalls, crop yields need to increase by more than is  
62 achievable at present by current crop improvement methods (Ray et al., 2013). It is  
63 also necessary to develop crops that are more stable in the face of increased  
64 climatic variability (Boyer et al., 2013). Hence, productivity combined with resilience  
65 is a sought-after goal. Improving crop performance under drought is complex  
66 because the effects of water availability on crop yield depend on crop developmental  
67 stage and genetic factors. The flowering period is particularly sensitive to drought  
68 (Boyer and Westgate, 2004); restriction of water at this time can decrease seed set,  
69 final seed number and harvested seed yield (Schussler et al., 1991a, b). Kernel  
70 abortion during drought at flowering can be alleviated by supplying sucrose to  
71 reproductive tissue (Zinselmeier, 1995a, b). Consequently, sucrose metabolism in  
72 reproductive tissue has been proposed as a target to alleviate the effects of drought  
73 during the reproductive period (Boyer and McLaughlin, 2007). Rather than directly  
74 targeting sucrose metabolism, it has been proposed that regulating the metabolism  
75 and utilisation of sucrose could be a more feasible target to alter assimilate  
76 partitioning (Boyer and McLaughlin, 2007).

77 The trehalose pathway is an important regulator of sucrose utilisation in plants  
78 (Schluepmann et al., 2003). Trehalose 6-phosphate (T6P), the precursor of  
79 trehalose, responds to sucrose likely as a signal of sucrose availability (Lunn et al.,  
80 2006; Martinez-Barajas et al., 2011; Nunes et al., 2013a; Yadav et al., 2014).  
81 Altering levels of T6P causes changes in gene expression (Nunes et al., 2013a),  
82 plant metabolism (Zhang et al., 2009; Figueroa et al., 2016) and growth (Nunes et  
83 al., 2013a), such that metabolic reprogramming occurs in light of sucrose availability.  
84 T6P can regulate starch levels through starch synthesis and breakdown (Kolbe et al.,  
85 2005; Martins et al., 2013) and enables the coordination of organic and amino acid  
86 metabolism with carbon availability (Figueroa et al., 2016). Such whole-scale effects  
87 are likely to be mediated by signal transduction and interaction with the feast/ famine  
88 protein kinase, SnRK1 (Zhang et al., 2009; Delatte et al., 2011; Nunes et al., 2013a,  
89 b; Tsai and Gazzarini, 2014). By mediating such effects on metabolism, growth and  
90 development, T6P ensures effective use of sucrose in addition to maintaining  
91 sucrose homeostasis. Yadav et al. (2014) have put forward a theory of the T6P:  
92 sucrose nexus; T6P levels could alter both the use and allocation of sucrose by  
93 increasing gene expression for the use of sucrose and mediating allocation by

94 perturbing sucrose homeostasis. There have been many reports of associations  
95 between the trehalose pathway and drought tolerance but no detailed mechanistic  
96 basis for such a correlation. The abundance of trehalose itself is too low to provide  
97 osmotic or oxidative stress protection against desiccation. Constitutive expression of  
98 trehalose pathway transgenes to alter T6P accumulation has produced examples of  
99 improved drought tolerance, but this may be because of reduced growth, which  
100 decreases water loss and improves survival, and does not improve productivity as is  
101 required in agriculture (Romero et al., 1997; Cortina and Cuiliane-Macia, 2005).

102 Nuccio et al. (2015) targeted changes in T6P abundance in reproductive  
103 tissue during the flowering period using a rice (*Oryza sativa*) *MADS6*: trehalose  
104 phosphate phosphatase (*OSMADS6: TPP1*) construct to alter sucrose metabolism  
105 for yield preservation during drought. This modification simultaneously decreased  
106 T6P and increased sucrose in female florets five days before pollination (Nuccio et  
107 al., 2015). In extensive field trials over several years and locations, the transgenic  
108 maize (*Zea mays*) demonstrated significantly improved yield, with and without  
109 drought during the flowering period, through enhanced kernel set. This provides one  
110 of very few reports wherein transgenic technology that has modified an intrinsic plant  
111 process has substantially improved yield and was reproducible in the field  
112 environment. Despite the importance of this success, little is known of the  
113 mechanistic details that underpin this yield improvement.

114 In the current study, we performed a detailed analysis of plants that were  
115 higher yielding than wild type in the field trials of Nuccio et al. (2015). We started  
116 from existing models of the mode of action of T6P through SnRK1. Reproductive  
117 tissue was sectioned into ear florets (female reproductive structures), pith (the  
118 vascular core of the ear), node (the vasculature in the stalk where the ear emerges)  
119 and shank (the branch where the ear attaches to the stalk). *OSMADS6: TPP1*  
120 expression was found to be associated with phloem tissue in these structures and  
121 transgene expression was greatest in florets and pith. Consistent with decreased  
122 T6P concentrations, primary metabolic pathways were downregulated and  
123 secondary metabolic pathways were upregulated in the tissues where *OSMADS6*  
124 promoter drove GUS expression. This altered the distribution in the component  
125 tissues of the reproductive structures away from pith toward the ear florets. *SWEET*  
126 genes were the only class of gene associated with assimilate transfer that were  
127 consistently affected in pith and florets. There were also changes in the expression

128 of SnRK1 marker genes, endogenous trehalose pathway genes and the gene  
129 encoding the SnRK1 beta subunit. Leaves of transgenic plants maintained higher  
130 rates of photosynthesis for longer during the reproductive period. Our results provide  
131 evidence that T6P/ SnRK1 acts as a central regulator of the balance between  
132 primary and secondary metabolism, assimilate distribution and the whole-plant  
133 source–sink interaction for crop yield improvement.

134

## 135 RESULTS

### 136 Expression of *OSMADS6: TPP1* During the Flowering Period

137 Female reproductive and leaf tissues were sampled for profiling analysis at 5-day  
138 intervals beginning at silk emergence, 5 days before pollination (-5), under controlled  
139 environmental conditions. Expression of *OSMADS6: TPP1* reached its highest levels  
140 in pith tissue compared to node, shank and floret (Fig. 1A, B). There were different  
141 *OSMADS6: TPP1* trends with respect to development in each tissue with expression  
142 increasing over time in shank and pith but decreasing over time in florets. Activity  
143 was most constant in the node during development. Analysis of *OSMADS6: GUS*  
144 shows *OSMADS6* expression localised to vasculature in all tissues, and phloem  
145 companion cells in particular (Fig. 2, Supplementary Fig. S1 and S2). Figure 1 shows  
146 that *OSMADS6: TPP1* transcript was detected in leaves but, when leaf tissue from  
147 *OSMADS6: GUS* plants was evaluated for GUS activity by histochemical analysis,  
148 no evidence of enzyme activity was found (Supplementary Fig. S1). Hence,  
149 *OSMADS6* does not appear to direct protein expression in leaves.

150

### 151 T6P and Trehalose

152 In wild-type reproductive tissue under well-watered (unstressed, US) conditions, T6P  
153 abundance ranged from 4 nmol g<sup>-1</sup> FW in the node, where it was most stable during  
154 development compared to other reproductive tissues, to 60 nmol g<sup>-1</sup> FW in the shank  
155 5 days before pollination (-5) (Fig. 3A). T6P then fell to less than 10 nmol g<sup>-1</sup> FW over  
156 the next 15 days (0, 5, 10). Overall during development, T6P levels were highest in  
157 florets and pith, between 32-60 nmol g<sup>-1</sup> FW and 11-30 nmol g<sup>-1</sup> FW, respectively.  
158 T6P levels in leaves were around 5 nmol g<sup>-1</sup> FW. In shank, the large peak of T6P 5  
159 days before pollination was increased by drought to 102 nmol g<sup>-1</sup> FW. Drought also  
160 increased T6P in pith, but decreased it at later time points in florets. *OSMADS6:*  
161 *TPP1* resulted in two- to threefold less T6P in pith and floret tissue under both well-

162 watered and drought conditions. The transgene barely affected T6P levels in node  
163 and leaves and increased T6P only twofold at the first time point in shank tissue.  
164 Trehalose content followed the same pattern as T6P for tissue type and  
165 developmental stage, with a 40 nmol g<sup>-1</sup> FW peak of trehalose in shank tissue at day  
166 -5 (Fig. 3C). Drought increased trehalose in node (Fig. 3D). *OSMADS6: TPP1* had  
167 little effect on trehalose, increasing it slightly in node but decreasing it in pith and  
168 florets. Trehalose was barely detectable in leaves.

169

### 170 **Metabolite Profiling**

171 The largest effects of *OSMADS6: TPP1* on metabolite profiles were found in floret  
172 and pith under well-watered and drought conditions (Fig. 4A, B, Supplementary Fig.  
173 3A, B), which coincided with the largest expression of transgene and largest effect of  
174 the transgene on T6P (Fig. 3A, B). The same trends were observed under well-  
175 watered and drought conditions. The changes in metabolites in floret and pith were  
176 largely in opposite directions, particularly for sucrose, glucose and fructose, and  
177 amino acids, which were increased in florets but decreased in pith, although amino  
178 acids in floret were unchanged or decreased at the last two time points. Levels of  
179 xylose and xylulose were decreased in both tissues. Adenosine monophosphate  
180 (AMP) increased in florets and decreased in pith in well-watered conditions.  
181 Contents of phospholipids, sphingolipids and sterols were increased in florets  
182 throughout development and were unchanged or decreased in pith. Node tissue was  
183 similar to pith with regard to amino acids, but dissimilar to pith for sugars which  
184 increased in node. Patterns of changes were less clear for shank and leaf, although  
185 leaves of transgenic plants had more carbohydrates than wild type. Allantoin was the  
186 only metabolite that increased in all tissues in transgenic plants. The known link  
187 between T6P and sucrose (Nunes et al., 2013a; Yadav et al., 2014) was broken in  
188 floret and node where a decrease in T6P (Fig. 3A, B) was related to more sucrose.  
189 Increased sucrose in leaves did not correspond to more T6P. In pith and shank,  
190 however, less T6P (Fig. 3A, B) was related to less sucrose (Supplementary Fig. 3A,  
191 B).

192

### 193 **Gene Expression**

194 Gene expression analysis from RNAseq analyses can be summarised by  
195 categorizing genes significantly increased or decreased in both transgenic lines

196 compared to wild type in all tissues under well-watered and drought conditions (Fig.  
197 5, Supplementary Tables S1-4). The Roast algorithm was used to identify  
198 biochemical pathways significantly perturbed (Fig. 6). Overall, transgenic pith tissue  
199 exhibited the greatest changes in gene expression due to transgene followed by  
200 floret, shank, node and leaf. There were no large differences between well-watered  
201 and drought conditions in numbers or types of genes affected. A total of 67 pathway  
202 categories were perturbed by the transgene in both events at two or more time  
203 points in at least one tissue in either unstressed or drought stressed plants (Fig. 6).  
204 Overall, expression of primary metabolic pathways (major flux e.g. sugar  
205 nucleotides, starch, cell wall, amino acids) was decreased, particularly in pith and  
206 floret, whereas expression of genes for secondary metabolic pathways (minor flux  
207 e.g. lipids, trehalose) was increased (Fig. 6).

208

### 209 **SnRK1 Marker Gene Expression**

210 Given the known effects of SnRK1 on metabolic pathways (Zhang et al., 2009;  
211 Figueroa et al., 2016), we quantified the extent of changes in SnRK1 marker gene  
212 expression previously identified in Baena-Gonzalez et al. (2007), Zhang et al. (2009),  
213 and Martinez-Barajas et al. (2011). Maize orthologues of *Arabidopsis* (*Arabidopsis*  
214 *thaliana*) genes reported to be regulated by SnRK1 were established using a  
215 combination of OrthoMCL, reciprocal best BLAST match and gene synteny (Li et al.,  
216 2003). Putative maize orthologues (183 induced markers, 242 repressed markers)  
217 are reported in Supplementary Tables S5A and S5B. Of those that changed in both  
218 lines on at least one time point, 23 orthologues of SnRK1 markers normally induced  
219 by SnRK1 were induced under unstressed conditions (US) in pith and 25 were  
220 induced under drought conditions (DS) (Fig. 7A). Also in pith, 14 maize orthologues  
221 of *Arabidopsis* genes reported to be repressed by SnRK1 were repressed in both  
222 events in at least one time point tested under unstressed conditions (US) and 19  
223 under drought conditions (DS) (Fig. 7B). Changes in SnRK1 markers were also  
224 observed in florets (Fig. 7A, Supplementary Table S5B).

225

### 226 **SnRK1 Activity and Gene Expression**

227 In unstressed plants, SnRK1 activities were higher in transgenic floret tissues  
228 compared to wild type at day 0 and day 10 (Fig. 8A, Supplementary Table S6). In  
229 pith, SnRK1 activity was higher in transgenics compared to wild type at day 10.

230 *SnRK1 $\beta$*  expression increased in transgenics compared to wild type in pith and floret  
231 tissue whereas expression of the gene encoding the SnRK1 AKIN11 subunit  
232 decreased in pith (Fig. 8B). SnRK1 activity was inhibited by T6P in floret and pith  
233 tissues (Fig. 8A). Combined with decreases in T6P (Fig. 3), it is likely that *in vivo*  
234 activities of SnRK1 were significantly higher in transgenics compared to wild type.

235

### 236 **Trehalose Pathway**

237 The endogenous trehalose biosynthetic pathway was one of the few biosynthetic  
238 pathways to be upregulated in transgenics compared to wild type (Fig. 6). The gene  
239 set defined by Henry et al. (2014) was analysed in more detail. There were large  
240 changes in pith and, to a lesser extent, florets (Fig. 9, Supplementary Table S7) in  
241 well-watered (US) and drought-stressed tissues (DS). Genes encoding class II  
242 trehalose phosphate synthase (TPS) and TPPB were induced in transgenics  
243 compared to wild type in well-watered and drought conditions, whereas *TPPA* was  
244 repressed. *TPS1* was also induced in pith.

245

### 246 **SWEET Genes**

247 We next sought to explain changes in the distribution of assimilate between pith and  
248 floret. We found that *SWEET* genes were the only class of genes involved in  
249 transport or efflux that had significantly altered expression levels (Fig. 10). Seven  
250 *SWEET* genes were upregulated across the reproductive tissue, with greatest  
251 changes in pith (Fig. 10, Supplementary Table S8). No significant changes in  
252 expression were found for genes encoding sucrose transporters; amino acid  
253 transporter gene expression decreased, whereas expression of genes for two nitrate  
254 transporters increased in pith (Fig. 11).

255

### 256 **Allantoinase**

257 Given the consistent change in allantoin levels in most of the transgenic samples,  
258 expression of genes involved in its metabolism was examined. Allantoinase, which  
259 metabolises allantoin to allantoate, was decreased in all tissue without drought  
260 except florets, and in all tissues under drought conditions (Fig. 11). Changes were  
261 compared to other genes putatively involved in nitrogen metabolism, none of which  
262 changed as consistently as allantoinase.

263



## 264 **Photosynthesis**

265 Rates of CO<sub>2</sub> uptake were determined in the leaf adjacent to the developing cob and  
266 the leaf above the developing ear under both well-watered and drought conditions.  
267 CO<sub>2</sub> uptake was up to 54% higher in transgenics compared to wild type (Fig. 12),  
268 with the largest percentage increase in primary leaf under drought (Fig. 12B). Effects  
269 were greatest at day 0 and day 5. There were no differences between transgenic  
270 and wild type in secondary leaves under drought (Fig. 12D). Analysis of gene  
271 expression in primary leaves showed upregulation of genes related to chloroplast  
272 and sucrose biosynthesis in unstressed tissue and decreases in chloroplast  
273 processes in drought-stressed leaves (Fig. 13).

274

## 275 **DISCUSSION**

276 Expression of a trehalose pathway gene linked to the rice *MADS6* promoter  
277 (*OSMADS6: TPP1*) in maize reproductive tissue was previously shown to increase  
278 maize yield in the field both with and without drought during the 2- to 3-week  
279 flowering period (Nuccio et al., 2015). This is one of the very few reports wherein  
280 genetically modifying an intrinsic process increases yield in field conditions. It is  
281 important to determine the biochemical and molecular basis of the yield increase to  
282 inform and develop crop improvement strategies. Four main conclusions can be  
283 drawn from this study. Firstly, localisation of *OSMADS6: TPP1* transgene expression  
284 in phloem cells of pith and florets lowered T6P levels two- to threefold. This resulted  
285 in the downregulation of primary metabolic pathways and upregulation of secondary  
286 metabolism, particularly lipid-related pathways, most strongly in pith. Secondly, this  
287 *OSMADS6: TPP1* transgene expression resulted in opposing changes in  
288 metabolites: increased sugars, amino acids and lipids in florets but decreased levels  
289 in pith; altered *SWEET* gene expression could account for assimilate transfer from  
290 pith towards floret. Allantoin was the only metabolite to increase in all tissues  
291 associated with the downregulation of allantoinase transcript in transgenic lines.  
292 Thirdly, a higher leaf photosynthetic rate in transgenics was likely to be in response  
293 to the enhanced movement of assimilate to florets. Fourthly, changes in SnRK1  
294 activity and in the expression of its subunit genes as well of SnRK1 marker genes  
295 and endogenous trehalose pathway genes implicate T6P/ SnRK1 as a central  
296 mechanism of assimilate partitioning, allocation and source-sink regulation in crops.

297

298 **Decreasing T6P in reproductive tissue downregulates primary metabolism and**  
299 **upregulates secondary metabolism, but causes distinct changes in metabolite**  
300 **profiles in component tissues**

301 Following the current thinking on the role of T6P in plants, a decrease in T6P would  
302 be expected to repress the biosynthetic activity of metabolic pathways (Zhang et al.,  
303 2009; Figueroa et al., 2016). This is observed in the reproductive tissues in this study  
304 with regard to primary metabolism (sugar nucleotide, amino acids, starch and cell  
305 wall, Fig. 6). However, an increase in the activity of the pathways of lipid  
306 biosynthesis was observed. This represents a refinement of the earlier hypothesis in  
307 that low T6P does not put a brake on all metabolic pathways but may stimulate  
308 secondary metabolism, lipids in this case, and hence produce qualitative changes in  
309 metabolism. Despite similarities in gene expression between component parts of  
310 reproductive tissue, metabolite profiles showed contrasting patterns in pith and  
311 florets, with pith having reduced assimilate content and floret increased assimilate  
312 content (Fig. 5A, B, Supplementary Fig. 3A, B). This may be explained because pith  
313 is composed of soft spongy parenchyma cells that store and transport nutrients to  
314 the developing florets, which are terminal sinks for assimilate. Hence, whilst  
315 reproductive tissue is an overall sink for assimilate, within the developing cob, pith is  
316 a source of assimilate for florets. Effects of T6P are likely to be highly context  
317 specific. This is evident in the different response of Arabidopsis seedlings compared  
318 to rosettes, which are mainly sink tissue and source tissue, respectively (Zhang et  
319 al., 2009; Wingler et al., 2012). Previous studies have shown an association of  
320 trehalose pathway gene expression with vasculature (Ramon et al., 2009) and the  
321 expression of *Attps1* is high in phloem companion cells (Genevestigator,  
322 <https://genevestigator.com/gv/>). Vascular expression of *TPS1* resulted in early  
323 flowering, suggesting a biological significance of the pathway in vascular tissue  
324 (Ruiz-Salas et al., 2016). This, combined with the T6P-associated changes to  
325 assimilate distribution in phloem cells found in this study suggest that T6P may  
326 regulate the flow of assimilates between tissues such as the pith and floret of maize  
327 reproductive structures. Regulation of *SWEET* genes could be a key factor in the  
328 regulation of T6P-mediated assimilate transfer as it was the only major class of  
329 protein associated with assimilate transfer to be consistently affected in this study  
330 (Fig. 10). Five *SWEET* genes were upregulated in pith, potentially implicating them in  
331 the movement of sucrose from pith to floret (Fig. 10); *SWEET* genes are proposed to

332 efflux sucrose to the phloem apoplasm (Braun et al., 2014). In particular, *SWEET13*,  
333 which was strongly affected in our study, has been previously singled out as a target  
334 for crop improvement in maize (Bezruczyk et al., 2017). In explaining elevated  
335 amino acids in florets in the absence of consistent upregulation of amino acid  
336 synthesis or amino acid transport genes, it is possible that increased sucrose  
337 availability may have resulted in more carbon skeleton for the synthesis of amino  
338 acids. Allantoin was the only metabolite to be increased consistently in all tissues  
339 (Supplementary Fig. 3A, B) found to be associated with a decrease in transcript for  
340 allantoinase (Fig. 11). Allantoin is associated with nitrogen assimilation in legumes  
341 and is considered a transport form of nitrogen (Coneva et al., 2014; Collier and  
342 Tegeder, 2012). It is possible that this may be associated with changes in amino  
343 acids, although the mechanistic basis of this is not known. Allantoin accumulation is  
344 associated with a number of traits involved in the tolerance of stresses, such as  
345 cadmium and salt, through antioxidant mechanisms (Brychkova et al., 2008), and  
346 jasmonic acid and ABA signalling (Takagi et al., 2016).

347

### 348 **Photosynthesis rate is maintained for longer in leaves of transgenics**

349 The normal developmental decline of photosynthesis in leaves was slowed in the  
350 transgenics (Fig. 12). Since there was no evidence of expression of the transgene in  
351 leaves, explanations for elevated photosynthesis must come from elsewhere. It is  
352 possible that greater movement of sucrose from pith into florets increased demand  
353 for sucrose, which maintained a higher photosynthetic rate for longer. Upregulation  
354 of a number of *SWEET* genes in reproductive tissue, including node and shank, (Fig.  
355 10) may have mediated the enhanced flow of sucrose from leaves. Sink regulation of  
356 photosynthesis has been a long-observed phenomenon (Paul and Foyer 2001).  
357 Recent work strongly implicates *SWEET* proteins in source–sink relationships in  
358 *Arabidopsis* (Durand et al., 2017). Sucrose levels in leaves of transgenics were also  
359 increased. This was consistent with increases in gene expression for sucrose  
360 biosynthesis and chloroplast processes in leaves (Fig. 13) and provides evidence of  
361 a wider role for T6P in source–sink relations regulating metabolism in sinks, which  
362 can provide feedforward regulation of leaf photosynthesis

363

### 364 **T6P/ SnRK1-mediated regulation**

365 A second part of the current model of T6P's mode of action is that SnRK1 mediates  
366 changes in gene expression associated with T6P abundance (Zhang et al., 2009;  
367 Nunes et al., 2013). To better understand whether SnRK1 could mediate the effects  
368 of lower T6P, expression of SnRK1 marker homologues was determined. Despite  
369 the fact that over the long term, direct cause-and-effect correlations are likely to be  
370 weakened by secondary and tertiary effects, there was evidence that changes in  
371 T6P resulted in altered regulation of gene expression through SnRK1 as the SnRK1  
372 marker genes normally induced by SnRK1 were induced (Fig. 7A) and those  
373 repressed by SnRK1 were more repressed than wild type (Fig. 7B). SnRK1 was also  
374 found to be inhibited by T6P and its activity, in the absence of T6P, was elevated in  
375 transgenic pith and florets (Fig. 8). These data provide *in vivo* and *in vitro* evidence  
376 of increased SnRK1 activity as a consequence of decreased T6P. This was  
377 associated with altered expression of the gene for the SnRK1 beta subunit, which  
378 may perform a regulatory rather than catalytic role within the SnRK1 complex  
379 (Baena-Gonzalez and Hanson 2017). Changes in *AKIN11* expression, which  
380 encodes the alpha subunit of the SnRK1 trimer were also found (Fig. 8). *AKIN11*  
381 expression has previously been shown to be altered in Arabidopsis with altered T6P  
382 (Schluepmann et al., 2004). Coincident with changes in SnRK1 was significantly less  
383 expression of endogenous trehalose pathway genes (Fig. 9). It was found previously  
384 that elevated T6P in Arabidopsis caused changes in expression of trehalose  
385 pathway genes, particularly class II TPSs (Zhang et al., 2009) in accordance with  
386 them being starvation inducible and sucrose repressible (Nunes et al., 2013a; Yadav  
387 et al., 2014). Here, these genes were induced in pith and induced to a lesser extent  
388 in florets. Our data confirm strong overlap and/or strong direct convergence between  
389 the SnRK1 and T6P signalling pathways, with the T6P inhibition of SnRK1 activity as  
390 a putative mechanism of metabolic reprogramming.

391 An association between T6P and sucrose is well established (Lunn et al.,  
392 2006; Nunes et al., 2013a). In this study, decreased T6P in transgenic pith correlated  
393 with less sucrose in pith, but less T6P in transgenic florets correlated with more  
394 sucrose. This confirms that the sucrose: T6P nexus (Yadav et al., 2014) is tissue  
395 dependent. The effect of T6P on the altered distribution and expression of *SWEET*  
396 genes implies a broader role of T6P in movement of sucrose between tissues.

397

## 398 **Summary**

399 The data in this study support a model wherein decreased T6P downregulates  
400 primary metabolism but upregulates secondary metabolism in the form of lipid  
401 synthesis. Low T6P resulted in different metabolite profiles in pith and floret with  
402 evidence that T6P regulates the movement of assimilate from pith to florets. This  
403 movement of sucrose may create extra demand for sucrose from leaves, giving rise  
404 to maintenance of high photosynthetic rates for longer. This indicates that T6P can  
405 regulate the balance between primary and secondary metabolism, the balance of  
406 assimilate accumulation within component parts of reproductive tissues and the  
407 activity of photosynthesis. Hence, changes in T6P in sinks can act as a major  
408 regulator of whole plant source/sink balance. Overall the changes in metabolite  
409 profiles and gene expression patterns in transgenics were similar under well-watered  
410 and drought conditions. This similarity indicates that these transgenics are  
411 predisposed to cope with drought and yield better under well-watered conditions by  
412 maintaining a source–sink balance that favours sucrose allocation to florets. Further,  
413 the data indicate that low T6P can upregulate secondary metabolism in the form of  
414 lipid synthesis. A strategy to target T6P in this way would improve both crop yields in  
415 different environments and produce qualitative changes in secondary metabolic  
416 pathways such as lipid biosynthesis.

417

## 418 **METHODS**

### 419 **Plant Material, Growth Conditions and Sampling**

420 Two independent transgenic lines (5217 and 5224) of maize (*Zea mays*) expressing  
421 the *OSMADS6: TPP1* construct, wild-type line A188 and *OSMADS6: GUS* were  
422 grown in a controlled environment ( $600 \mu\text{mol m}^{-2} \text{s}^{-1}$ , 16 h day, 80/70% relative  
423 humidity day/night, 27°C/21°C day/night in Rothamsted compost supplemented with  
424 full nutrition as in Nuccio et al., 2015). Five different tissue types from female  
425 reproductive tissue (florets, shank, pith, node and fully expanded leaf next to the  
426 developing cob) were sampled at 5-day intervals at four time points, 5 days before  
427 pollination to 10 days after pollination (labelled as 1, 2, 3, 4; corresponding to -5, 0,  
428 5, 10 days relative to pollination). Five biological replicates from individual plants  
429 were taken for each line, time and tissue. Tissue was sampled during the middle of  
430 the photoperiod, snap frozen in liquid N<sub>2</sub> and stored at -80°C until analysis. Plants  
431 were grown under full irrigation, or with drought imposed 5 days before the first  
432 sampling point by withholding water until pots reached 65% of the weight before

433 withholding water, as in Nuccio et al. (2015). This level of drought was maintained  
434 throughout the sampling period by weighing plants daily. *OSMADS6: GUS*  
435 expression cassette activity was assessed by histochemical localisation of  $\beta$ -  
436 glucuronidase (GUS) protein (described in Nuccio et al., 2015).

437

#### 438 **RNA seq**

439 Total RNA was extracted from 100 mg ground maize tissue using the Ribopure™ Kit  
440 (Ambion®) according to the manufacturer's instructions. RNA was quantified using a  
441 Nanodrop and RNA integrity quality was checked by Agilent RNA 6000 Nano Kit®  
442 (Agilent Technology™) according to the manufacturer's instructions.

443 Sequence libraries were prepared at Syngenta and samples were sequenced  
444 on a HiSeq2000 by GeneWiz. FastQ sequence files were examined by FastQC  
445 software (v0.11.2). Raw reads were used for mapping to the maize reference  
446 genome 5a57 (AGP\_v2) with gene models 5b.60 (www.maizegdb.org). Tophat  
447 (v2.0.12) with bowtie2 (version 2.2.3) was used for read alignment (Trapnell, 2009;  
448 Langmead, 2009). The maximum read mismatches allowed were six. Reads which  
449 mapped to more than six places were randomly reported to six mapped locations.  
450 Counts were generated from alignment files in BAM format using a custom Python  
451 script. Briefly, the method produces counts for gene regions that are defined by a  
452 gene feature file (gff3 format) for reads aligning to that region. If a given read aligned  
453 to multiple genomic regions defined as genes, up to six regions received one count  
454 each. If the read aligned to more than six genomic loci defined as genes, then the  
455 read was discarded. This method avoided loss of useful information in cases where  
456 reads aligned equally well to different genes. The annotation file used for gene count  
457 generation was customized to include sequences for the trait gene *Tpp1* and the  
458 phosphomannose isomerase (PMI) selectable marker gene used in transformation,  
459 as well as maize mitochondria and chloroplast sequences. A further step included  
460 filtering by raw counts before any normalization. Genes were only kept if they had a  
461 'counts per million' value of 10 or more in at least three different samples which  
462 resulted in a total of 22,714 and 22,748 features (genes) reported for the unstressed  
463 and drought studies, respectively.

464 Read quality was analysed using FastQC  
465 (<http://www.bioinformatics.babraham.ac.uk/projects/fastqc/>). Most of the samples  
466 had fairly similar GC content, consistent with the GC content of the Maize genome.

467 To correct for possible GC or length bias, data were normalized using the EDASeq R  
468 package (Risso, 2011). Differential expression analysis and gene ontology (GO)  
469 term and pathway enrichment analyses were conducted using the EdgeR package  
470 (Robinson et al., 2010).

### 471 **GO term and Pathway Enrichment Analysis**

472 Gene expression analysis from RNAseq was summarised into genes significantly  
473 increased or decreased in both transgenic lines compared to wild type in all tissues  
474 under well-watered and drought conditions (Fig. 4, Fig. 6, Supplementary Tables S1-  
475 4). Genes were considered to be differentially expressed if results of statistical tests  
476 had a false discovery rate of less than 0.05 and the effect size, measured as  
477 absolute value of log<sub>2</sub> fold change, was greater than one. The experimental design  
478 resulted in a total of 80 contrasts of transgenic lines compared to wild type controls  
479 across the five tissue types, four time points and different watering regimes. Initial  
480 contrasts compared individual transgenic events to wild type controls. Roast  
481 implemented in the EdgeR package was used for enrichment of GO terms and sets  
482 of genes predicted to code for enzymes in biochemical pathways (Wu et al., 2010).  
483 Roast uses a gene set test that assigns a P-value to a set of genes as a unit, which  
484 increases statistical power for interpreting results compared with other available  
485 permutation tests or more traditional methods such as Fisher's Exact tests for gene  
486 set enrichment. Gene sets of biochemical pathways and GO terms were assembled  
487 from data obtained from the Maize Genetics and Genomics Database  
488 ([www.maizeGDB.org](http://www.maizeGDB.org)). For pathway data, BioPax formatted files were downloaded  
489 from MaizeCyc2.0.1 and parsed to get all gene models likely encoding enzymes in  
490 all maize biochemical pathways and reactions in the data set. These data and GO  
491 annotations were formatted into files suitable for use with Roast using ad hoc scripts.  
492 Data from mRoast, a version of Roast for multiple gene sets, included multiple test  
493 corrected P-values (False Discovery Rate (FDR)) as well as directionality of change  
494 of the majority of genes within a defined gene set. For Figure 6, data were  
495 condensed by first only reporting pathways significantly enriched (false discovery  
496 rate of < 0.05) in the same direction by both transgenic events in a particular time  
497 point and tissue. This was done for both unstressed and drought stressed plants.  
498 Secondly, pathways were only reported if they were significantly perturbed in the  
499 same direction in both transgenic events in at least two of the four time points tested.

500 These pathway results were further condensed using the pathway ontology in  
501 MaizeCyc2.0.1. Individual pathways were grouped together into higher order  
502 biochemical pathways using these ontologies. Only pathways included in this  
503 ontology were included, all individual reactions enriched in the data set were  
504 eliminated. In cases where multiple pathways were present under a given pathway  
505 ontology, a single pathway was chosen as most representative of the pathway  
506 category.

507

### 508 **Metabolite Analysis**

509 All extraction and analysis was conducted at Metabolon. Samples were extracted  
510 and split into equal parts for analysis on GC/MS and LC/MS/MS platforms.  
511 Proprietary software was used to match ions to an in-house library of standards for  
512 metabolite identification and quantitation by peak area integration. LC/MS was based  
513 on a Waters ACQUITY UPLC and a Thermo-Finnigan LTQ mass spectrometer  
514 consisting of an electrospray ionization (ESI) source and linear ion-trap (LIT) mass  
515 analyzer. The sample extract was split into two aliquots, dried, then reconstituted in  
516 acidic or basic LC-compatible solvents, each of which contained 11 or more injection  
517 standards at fixed concentrations. One aliquot was analyzed using acidic positive ion  
518 optimized conditions and the other using basic negative ion optimized conditions in  
519 two independent injections using separate dedicated columns. Extracts reconstituted  
520 in acidic conditions were gradient eluted using water and methanol both containing  
521 0.1% formic acid, while the basic extracts, which also used water/methanol,  
522 contained 6.5 mM ammonium bicarbonate. The MS analysis alternated between MS  
523 and data-dependent MS2 scans using dynamic exclusion. Samples for GC/MS  
524 analysis were re-dried under vacuum desiccation for a minimum of 24 h prior to  
525 being derivatized under dried nitrogen using bistrimethyl-silyl-trifluoroacetamide  
526 (BSTFA). The GC column was 5% phenyl and the temperature ramp 40°C to 300°C  
527 over 16 min. Samples were analyzed on a Thermo-Finnigan Trace DSQ fast-  
528 scanning single-quadrupole mass spectrometer using electron impact ionization. The  
529 instrument was tuned and calibrated for mass resolution and mass accuracy daily.  
530 The information output from the raw data files was automatically extracted as  
531 discussed below. Accurate mass determination (LC/MS) and MS/MS fragmentation  
532 (LC/MS/MS) for structural elucidation was based on a Waters ACQUITY UPLC and a  
533 Thermo-Finnigan OrbiElite mass spectrometer, which had an LIT front end and an



534 orbitrap mass spectrometer back end. Accurate mass measurements could be made  
535 on the parent ion as well as fragments. The typical mass error was less than 5 ppm.

536 The informatics system consisted of four major components, the Laboratory  
537 Information Management System (LIMS), the data extraction and peak-identification  
538 software, data processing tools for QC and compound identification, and a collection  
539 of information interpretation and visualization tools for use by data analysts. The  
540 hardware and software foundations for these informatics components were the LAN  
541 backbone, and a database server running Oracle 10.2.0.1 Enterprise Edition. Peaks  
542 were identified using Metabolon's proprietary peak integration software, and  
543 component parts were stored in a separate and specifically designed complex data  
544 structure. Compounds were identified by comparison to library entries of purified  
545 standards or recurrent unknown entities.

546 For statistical analysis pair-wise comparisons using Welch's T-tests and/or  
547 Wilcoxon's rank sum tests were performed. ANOVA was also conducted.  
548 Metabosync (Metabolon Inc, Durham, NC, USA) was used to show changes in  
549 metabolite abundance in representative contrasts of transgenic event 5224  
550 compared to wild type grown in unstressed conditions to show the full extent of  
551 metabolite changes using Welch's T-tests to calculate the size of the circle and  
552 statistical significance of difference of mean values (Fig. 5A, B).

553

### 554 **SnRK1 Activity**

555 Total soluble protein was extracted from 200 mg of tissue ground under liquid  
556 nitrogen in a pestle and mortar in 600  $\mu$ L of ice-cold homogenization buffer of 100  
557 mM tricine-NaOH, pH 8, 25 mM NaF, 5 mM dithiothreitol, 2 mM tetrasodium  
558 pyrophosphate, 0.5 mM EDTA, 0.5 mM EGTA, 1 mM benzamidine, 1 mM  
559 phenylmethylsulfonyl fluoride, 1 mM protease inhibitor cocktail (Sigma P9599),  
560 phosphatase inhibitors (PhosStop; Roche) and insoluble polyvinylpyrrolidone to 2%  
561 (w/v). Homogenate was centrifuged at 13,000g at 4°C. Supernatant (250  $\mu$ L) was  
562 desalted in illustra NAP-5 columns (GE Healthcare) pre-equilibrated with  
563 homogenization buffer. Eluent was supplemented with protease inhibitor cocktail and  
564 okadaic acid to 2.5 mM before freezing in liquid nitrogen. SnRK1 activity of three  
565 replicates for each time point was determined as described by Zhang et al. (2009) in  
566 a final volume of 25  $\mu$ l in microtitre plate wells at 30°C. Assay medium was 40 mM

567 HEPES-NaOH, pH 7.5, 5 mM MgCl<sub>2</sub>, 200 mM ATP containing 12.5 kBq [ $\gamma$ -<sup>33</sup>P] ATP  
568 (PerkinElmer), 200  $\mu$ M AMARA peptide (Enzo Life Sciences, UK, Ltd), 5 mM  
569 dithiothreitol, 1  $\mu$ M okadaic acid and 1 mM protease inhibitor cocktail (Sigma P9599).  
570 Assays were started with 5  $\mu$ L extract and stopped after 6 min by transferring 15  $\mu$ L  
571 to 4 cm<sup>2</sup> squares of Whatman P81 phosphocellulose paper immersed immediately in  
572 1% phosphoric acid. These were then washed with four 800 ml volumes of 1%  
573 phosphoric acid, immersed in acetone for 15 min, air dried and transferred to vials  
574 with 3.5 ml of scintillation cocktail (Ultima Gold).

575

### 576 **Photosynthesis**

577 Leaf gas exchange measurements of well-watered and water-stressed maize plants  
578 were carried out using a portable infra-red open gas exchange system (LI-6400XT;  
579 LI-COR, Lincoln, USA) under the growing conditions (ambient CO<sub>2</sub> (400  $\mu$ l l<sup>-1</sup>), leaf  
580 temperature 27°C, photosynthetic photon flux density 600  $\mu$ mol m<sup>-2</sup> s<sup>-1</sup>, relative air  
581 humidity 65  $\pm$  5%. Each leaf reached a steady state of CO<sub>2</sub> uptake in the leaf  
582 chamber before measurements were taken.

### 583 **ACCESSION NUMBERS**

584 Maize SnRK1 gene accession numbers: SnRK1beta, GRMZM2G025459; AKINB,  
585 GRMZM2G138814; AKIN10B, GRMZM2G077278; AKIN10, GRMZM2G077278;  
586 AKIN11, GRMZM2G107867.

587 Maize trehalose pathway gene accession numbers: TPPA1, GRMZM2G178546;  
588 TPPB1.3, GRMZM2G174396; TPPA.3, GRMZM2G112830; TPPB.1.2,  
589 GRMZM2G140078; TPPB.1.4, GRMZM2G055150; TPSII.3.2, GRMZM2G123277;  
590 TPSII.4.2, GRMZM2G008226; TPSII.4.1GRMZM2G527891; TPSII.2.1,  
591 GRMZM2G019183; TPSII.5.4, GRMZM2G122231; TPSII.4.3, GRMZM2G366659;  
592 TPSII.5.3, GRMZM2G312521; TPPB.2.1, GRMZM2G014729.

593 Maize SWEET gene accession numbers: SWEET1b, GRMZM2G153358; SWEET2,  
594 GRMZM2G324903; SWEET3a, GRMZM2G179679; SWEET11, GRMZM2G368827;  
595 SWEET13a, GRMZM2G173669; SWEET13c, GRMZM2G179349; SWEET14b,  
596 GRMZM2G015976; SWEET15a, GRMZM2G168365; SWEET15b,  
597 GRMZM5G972392; SWEET16, GRMZM2G107597.

598 Maize allantoinase gene accession number: GRMZM2G173413.

599 RNAseq Accession: PRJNA421180 ID: 421180; Unstressed samples: SUB3315967;  
600 Drought Stressed Samples: SUB3357197  
601 <https://www.ncbi.nlm.nih.gov/bioproject/PRJNA421180>

602

## 603 **SUPPLEMENTAL DATA**

604 **Supplementary Figure S1. Histochemical analysis of *OSMADS6: GUS*.**

605 **Supplementary Figure S2. Histochemical analysis of *OSMADS6: GUS* activity**  
606 **in node.**

607 **Supplementary Figure S3. Effect of *OSMADS6: TPP1* on selected metabolites**  
608 **in reproductive tissues and leaves during early reproductive development.**

609 **Supplementary Table S1. Changes in gene expression.**

610 **Supplementary Table S2. Changes in gene expression.**

611 **Supplementary Table S3. Changes in gene expression.**

612 **Supplementary Table S4. Changes in gene expression.**

613 **Supplementary Table S5. SnRK1 marker gene expression previously identified**  
614 **in Baena-Gonzalez et al. (2007); Zhang et al. (2009); Martinez-Barajas et al.**  
615 **(2011) in transgenics compared to wild type.**

616 **Supplementary Table S6. SnRK1 gene expression in transgenics compared to**  
617 **wild type.**

618 **Supplementary Table S7. Trehalose pathway gene expression in transgenics**  
619 **compared to wild type.**

620 **Supplementary Table S8. SWEET gene expression in transgenics compared to**  
621 **wild type.**

622

## 623 **ACKNOWLEDGEMENTS**

624 Rothamsted Research receives strategic funding from the Biotechnological and  
625 Biological Sciences Research Council of the UK. MJP acknowledges support from  
626 the Designing Future Wheat Institute Strategic Programme (BB/P016855/1).

627

628 **FIGURE LEGENDS**

629 **Figure 1. *OSMADS6: TPP1* expression in reproductive tissues and leaves**  
630 **during early reproductive development.**

631 Data are from (A) unstressed and (B) drought-stressed plants. Normalized gene  
632 count data are plotted for each transgenic event (5217 or 5224) and the wild-type  
633 (WT) A188 line. The horizontal line in each box indicates the mean. Vertical lines  
634 indicate the range for each sample. The time points are 5 days before pollination (-  
635 5), day of pollination (0), 5 days after pollination (5) and 10 days after pollination  
636 (10). Data are the mean +/- SD of 5 biological replicates.

637

638 **Figure 2. Histochemical localization of  $\beta$ -glucuronidase activity produced by**  
639 **the *OSMADS6: GUS* reporter gene in unstressed maize during early**  
640 **reproductive development.**

641 Samples were collected from (A-D) ear florets, (E-H) shank, (I-L) node, (M-N) shank  
642 at high magnification, (O) node at high magnification, (P) pith at high magnification.  
643 Samples were collected at 5 days before pollination (A, E, I, M), day of pollination (B,  
644 F, J, N), 5 days after pollination (C, G, K, O) and 10 days after pollination (D, H, L,  
645 P). Samples were incubated in the histochemical reagent and cleared as described  
646 in the Methods. Xylem and phloem cells are indicated by the red arrows.

647

648 **Figure 3. Effect of the *OSMADS6: TPP1* on T6P and trehalose in reproductive**  
649 **tissues and leaves during early reproductive development.**

650 Samples were collected from (A, C) unstressed and (B, D) drought-stressed plants  
651 at 5 days before pollination (-5), day of pollination (0), 5 days after pollination (5) and  
652 10 days after pollination (10). Vertical lines indicate the range for each sample. Data  
653 are the mean  $\pm$  SD (n=5).

654

655 **Figure 4.** Screen shot from Metabosync showing change in metabolite abundance  
656 in response to *OSMADS6: TPP1*. Representative contrasts of transgenic event 5224  
657 compared to wild type grown in unstressed conditions to show full extent of  
658 metabolite changes. **A.** Floret tissue at day of pollination. **B.** Pith tissue 5 days after  
659 pollination. Biochemicals shown are key metabolites in aromatic amino acid  
660 metabolism, glutamate family amino acid synthesis, phospholipid metabolism,

661 sucrose metabolism, aspartate family amino acid synthesis, arginine biosynthesis,  
662 BCAA metabolism, trehalose biosynthesis and nitrogen metabolism. Circles  
663 represent metabolites as labeled. The size of the circle indicates statistical  
664 significance of difference of mean values from Welch's T-tests. Blue indicates fold  
665 change (ratio of mean value from all replicates in samples of transgenic event/  
666 wild type) of less than one and red indicates fold change of greater than one.

667

668 **Figure 5.** Genes significantly upregulated or downregulated in different tissues in  
669 both *OSMADS6: TPP1* transgenic lines compared to wild type in well-watered  
670 conditions and under drought. The time points are 5 days before pollination (1), day  
671 of pollination (2), 5 days after pollination (3), and 10 days after pollination (4)

672

673 **Figure 6. *OSMADS6: TPP1* effect on biochemical pathways.** Transcript profiling  
674 data from both the 5217 and 5224 events were compared to wild type (A188) to  
675 identify significantly perturbed biochemical pathways. A white cell indicates pathways  
676 that were not affected and a dark cell (red, up; blue, down) indicates pathways that  
677 were significantly affected by the transgene. The data are from unstressed (US) and  
678 drought stressed (DS) plants. Results from the four time points were condensed by  
679 only reporting pathways significantly affected in at least two time points.

680

681 **Figure 7. Heat map showing the effect of *OSMADS6: TPP1* on SnRK1-regulated**  
682 **genes.** Maize orthologues of Arabidopsis/ wheat genes shown to be **(A)** induced or  
683 **(B)** suppressed by SnRK1 in Arabidopsis/ wheat (Zhang et al., 2009; Martinez-  
684 Barajas et al., 2011) were examined using differential expression analysis from  
685 unstressed (US) or drought-stressed (DS) plants between wild type and transgenic  
686 lines 5217 and 5224. Red indicates upregulation and blue indicates downregulation  
687 relative to wild type (A188). White indicates no significant (NS) difference and grey  
688 indicates no data. The time points are 5 days before pollination (1), day of pollination  
689 (2), 5 days after pollination (3) and 10 days after pollination (4).

690

691 **Figure 8. Effect of *OSMADS6: TPP1* on SnRK1 activity and gene expression.**

692 Pith and floret tissues were examined for **(A)** extractable SnRK1 activity (line 5127)  
693 and **(B)** differential expression of maize orthologues of Arabidopsis genes that  
694 encode SnRK1 subunits between wild type and transgenic line 5217 and 5224.

695 SnRK1 activity was assayed in the presence and absence of 1 mM T6P. Data are  
696 the mean  $\pm$  SD (n = 3). The time points are 5 days before pollination (1), day of  
697 pollination (2), 5 days after pollination (3) and 10 days after pollination (4).

698

699 **Figure 9. Effect of *OSMADS6: TPP1* on trehalose metabolism gene expression.**

700 Differential expression analysis of trehalose-6-phosphate synthase (TPS) and  
701 trehalose-6-phosphate phosphatase (TPP) gene family members between wild type  
702 and transgenic lines 5217 and 5224. The time points are 5 days before pollination  
703 (1), day of pollination (2), 5 days after pollination (3) and 10 days after pollination (4).

704

705 **Figure 10. Heat map showing the effect of *OSMADS6: TPP1* on SWEET genes.**

706 Heat maps represent differential expression analysis between wild type and  
707 transgenic lines 5217 and 5224. The time points are 5 days before pollination (1),  
708 day of pollination (2), 5 days after pollination (3) and 10 days after pollination (4).

709

710 **Figure 11. Heat map showing allantoinase and nitrogen transport and  
711 metabolic processes.** Heat maps represent differential expression analysis  
712 between wild type and transgenic lines 5217 and 5224. The time points are 5 days  
713 before pollination (1), day of pollination (2), 5 days after pollination (3) and 10 days  
714 after pollination (4).

715

716 **Figure 12. Rates of photosynthesis during 2-week flowering period.**

717 Wild type (open symbols) and *OSMADS6: TPP1* transgenic line 5224 (closed  
718 symbols). **(A, B)** the leaf next to the ear and **(C, D)** the leaf above the ear.  
719 Unstressed **(A, C)** and drought stressed **(B, D)**. Time points are 5 days before  
720 pollination (1), day of pollination (2), 5 days after pollination (3), 10 days after  
721 pollination (4). Rates of CO<sub>2</sub> uptake were measured under the growing conditions  
722 (ambient CO<sub>2</sub> (400  $\mu$ l l<sup>-1</sup>), leaf temperature 27°C, photosynthetic photon flux density  
723 600  $\mu$ mol m<sup>-2</sup> s<sup>-1</sup>, relative air humidity 60  $\pm$  5%. Data are the mean  $\pm$  SD (n = 4). \*  
724 indicates statistical significance between transgenic and wild type at  $p < 0.05$ .

725

726 **Figure 13. Heat map showing photosynthesis genes in mature leaves.**

727 Heat maps represent differential expression analysis between wild type and  
728 transgenic lines 5217 and 5224. The time points are 5 days before pollination (1),  
729 day of pollination (2), 5 days after pollination (3) and 10 days after pollination (4).

730

731

732 **LITERATURE CITED**

- 733 **Baena-Gonzalez E, Rolland F, Thevelein JM, Sheen J** (2007) A central integrator  
734 of transcription networks in plant stress and energy signalling. *Nature* 448, 938-942
- 735 **Baena-Gonzalez E, Hanson J** (2017) Shaping plant development through the  
736 SnRK-TOR metabolic regulators. *Current Opinion in Plant Biology* 35, 152-157
- 737 **Bezruczyk M, Hartwig T, Horshman M, Nian Char S, Yang J, Yang B, Frommer  
738 WB, Sosso D** (2017) Impaired phloem loading in genome-edited triple knock-out  
739 mutants of SWEET13 sucrose transporters. *Biorxiv* doi.org/10.1101/197921
- 740 **Boyer JS, McLaughlin JE** (2007) Functional reversion to identify controlling genes  
741 in multigenic responses: analysis of floral abortion. *J Exp Bot* 58: 267–277
- 742 **Boyer JS, Westgate ME** (2004) Grain yields with limited water. *J Exp Bot* 55: 385–  
743 2394
- 744 **Boyer J, Byrne P, Cassman K, Cooper M, Delmer D, Greene T, et al.** (2013) The  
745 US drought of 2012 in perspective: A call to action. *Global Food Security* 2:139-43
- 746 **Braun DM, Wang L, Ruan Y-L** (2014) Understanding and manipulating sucrose  
747 phloem loading, unloading, metabolism, and signalling to enhance crop yield and  
748 food security. *Journal of Experimental Botany* 65, 1713–1735
- 749 **Brychkova G, Alikulov Z, Fluhr R, Sagi M** (2008) A critical role for ureides in dark  
750 and senescence-induced purine remobilization is unmasked in the *Atxdh1*  
751 *Arabidopsis* mutant. *Plant Journal* 54: 496-509
- 752 **Chen THH, Murata N** (2002) Enhancement of tolerance of abiotic stress by  
753 metabolic engineering of betaines and other compatible solutes. *Current Opinion in*  
754 *Plant Biology* 5, 250-257
- 755 **Chen LQ, Hou BH, Lalonde S, Takanaga H, Hartung ML, Qu XQ, et al.** (2010)  
756 Sugar transporters for intercellular exchange and nutrition of Pathogens. *Nature* 25:  
757 527-532
- 758 **Collier, R and Tegeder M** (2012) Soybean ureide transporters play a critical role in  
759 nodule development, function and nitrogen export. *Plant J* 72: 355-367
- 760 **Cortina C, Culiáñez-Macià FA** (2005) Tomato abiotic stress enhanced tolerance by  
761 trehalose biosynthesis. *Plant Sci* 169: 75–82
- 762 **Delatte TL, Sedijani P, Kondou Y, Matsui M, de Jong GJ, Somsen GW, Wiese-  
763 Klinkenberg A, Primavesi LF, Paul MJ, Schluemann H** (2011) Growth arrest by  
764 trehalose-6-phosphate: an astonishing case of primary metabolite control over  
765 growth by way of the SnRK1 signaling pathway. *Plant Physiology* 157: 160-174



766

767 **Durand M, Mainson D, Porcheron B, Maurousset L, Lemoine R, Portau N** (2017)  
768 Carbon source-sink relationship in *Arabidopsis thaliana*: the role of sucrose  
769 transporters. *Planta* doi.org/10.1007/s00425-017-2807-4

770 **Figueroa CM, Feil R1, Ishihara H, Watanabe M, Kölling K, Krause U, Höhne M,**  
771 **Encke B, Plaxton WC, Zeeman SC, Li Z, Schulze WX, Hoefgen R, Stitt M, Lunn**  
772 **JE** (2016) Trehalose 6-phosphate coordinates organic and amino acid metabolism  
773 with carbon availability. *Plant J* 85: 410-423

774 **Habben JE, Bao X, Bate NJ, Debruin JL, Dolan D, Hasegawa D, et al.** (2014)  
775 Transgenic alteration of ethylene biosynthesis increases grain yield in maize under  
776 field drought-stress conditions. *Plant Biotechnol J* 12: 685-93

777 **Henry C, Bledsoe SW, Siekman A, Kollman A, Waters BM, Feil R, Stitt M,**  
778 **Lagrimini LM** (2014) The trehalose pathway in maize: conservation and gene  
779 regulation in response to the diurnal cycle and extended darkness. *J Ex Bot* 65:  
780 5959-5973

781 **Kolbe A, Tiessen A, Schluepmann H, Paul MJ, Ulrich S, Geigenberger P** (2005)  
782 Trehalose 6-phosphate regulates starch synthesis via post-translational activation of  
783 ADP-glucose pyrophosphorylase. *Proceedings of the National Academy of*  
784 *Sciences USA* 102, 11118-11123

785 **Langmead B, Trapnell C, Pop M, Salzberg SL** (2009) Ultrafast and memory-  
786 efficient alignment of short DNA sequences to the human genome. *Genome Biology*  
787 10: R25 DOI: 10.1186/gb-2009-10-3-r25

788 **Li L, Stoeckert J, Roos DS** (2003) OrthoMCL: Identification of Ortholog Groups for  
789 Eukaryotic Genomes. *Genome Research* 13: 2178-2189

790 **Lunn JE, Feil R, Hendriks JH, Gibon Y, Morcuende R, Osuna D, Scheible WR,**  
791 **Carillo P, Hajirezaei MR, Stitt M** (2006) Sugar-induced increases in trehalose 6-  
792 phosphate are correlated with redox activation of ADPglucose pyrophosphorylase  
793 and higher rates of starch synthesis in *Arabidopsis thaliana*. *Biochem J* 397: 139-148

794 **Martínez-Barajas E, Delatte T, Schluepmann H, de Jong GJ, Somsen GW,**  
795 **Nunes C, Primavesi LF, Coello P, Mitchell RAC, Paul MJ** (2011) Wheat grain  
796 development is characterised by remarkable T6P accumulation pre-grain filling:  
797 tissue distribution and relationship to SNF1-related protein kinase1 activity. *Plant*  
798 *Physiology* 156: 373-381

799 **Martins MCM, Hejazi M, Fettke J, Steup M, Feil R, Krause U, Arrivault S, Vosloh**  
800 **D, Figueroa CM, Ivakov A, Yadav UP, Piques M, Metzner D, Stitt M, Lunn JE**  
801 (2013) Feedback inhibition of starch degradation in arabidopsis leaves mediated by  
802 trehalose 6-phosphate. *Plant Physiology* 163: 1142-1163

803 **Nuccio ML, Wu J, Mowers R, Zhou H-P, Meghji M, Primavesi LF, et al.** (2015)  
804 Expression of trehalose 6-phosphate phosphatase in maize ears improves yield in  
805 well-watered and drought conditions. *Nature Biotechnol* 33: 862-874

806 **Nunes C, O'Hara, Primavesi LF, Delatte TL, Schluempmann H, Somsen GW, et**  
807 **al.,** (2013a) The T6P/ SnRK1 signaling pathway primes growth recovery following  
808 relief of sink limitation. *Plant Physiol* 162: 1720-1732

809 **Nunes C, Primavesi LF, Patel MK, Martinez-Barajas E, Powers SJ, Sagar R,**  
810 **Feverheiro PS, Davis BG, Paul MJ** (2013b) Inhibition of SnRK1 by metabolites:  
811 tissue-dependent effects and cooperative inhibition by glucose 1-phosphate in  
812 combination with trehalose 6-phosphate. *Plant Physiology and Biochemistry* 63: 89-  
813 98

814 **Paul MJ, Nuccio ML, Basu SS** (2017) Are GM crops for yield and resilience  
815 possible? *Trends in Plant Science* doi.org/10.1016/j.tplants.2017.09.007

816 **Pellny TK, Ghannoum O, Conroy JP, Schluempmann H, Smeekens S, Andralojc**  
817 **J, Krause K-P, Goddijn O, Paul MJ** (2004) Genetic modification of photosynthesis  
818 with, *E. coli* genes for trehalose synthesis. *Plant Biotechnol J* 2: 71-82

819 **Ramon M, de Smet I, Vanesteene L, Naudts M, Leyman B, Van Dijck P, Rolland**  
820 **F, Beekman T, Thevelein JM** (2009) Extensive expression regulation and lack of  
821 heterologous enzymatic activity of the Class II trehalose metabolism proteins from  
822 *Arabidopsis thaliana*. *Plant Cell and Environment* 32, 1015-1032

823 **Ray DK, Mueller ND, West PC, Foley JA** (2013) Yield trends are insufficient to  
824 double global crop production by 2050. *PLoS ONE*. 8: e66428

825 **Risso D, Schwart K, Sherlock G, Dudoit S** (2011) GC-Content Normalization for  
826 RNA-Seq Data. *BMC Bioinformatics* 12:480

827 **Robinson MD, McCarthy DJ, Smyth GK** (2010) edgeR: A Bioconductor package  
828 for differential expression analysis of digital gene expression data. *Bioinformatics* 26,  
829 139-140

830 **Romero C, Belles JM, Vaya JL, Serrano R, Cullianez-Macia FA** (1997) Expression  
831 of the yeast trehalose-6-phosphate synthase gene in transgenic tobacco plants:  
832 pleiotropic phenotypes include drought tolerance. *Planta* 201: 293–297

833 **Ruiz-Salas, J-L, Ruiz-Medrano, R, Montes-Horcasitas, MC, Agreda-Laguna, KA,**  
834 **Hinojosa-Moya, J, Xoconostle-Cazares, B** (2016) Vascular expression of trehalose  
835 phosphate synthase1 (TPS1) induces flowering in Arabidopsis. *Plant Omics* 9: 344-  
836 351

837 **Schluepmann H, Pellny T, van Dijken A, Smeekens S, Paul MJ** (2003) Trehalose  
838 6-phosphate is indispensable for carbohydrate utilisation and growth in Arabidopsis  
839 thaliana. *Proceedings of National Academy of Sciences* 100: 6849-6854

840 **Schluepmann H, van Dijken A, Aghdasi M, Wobbes B, Paul M, Smeekens S**  
841 (2004) Trehalose-mediated growth inhibition of Arabidopsis seedlings is due to  
842 trehalose-6-phosphate accumulation. *Plant Physiology*: 135, 879-890

843 **Schussler JR, Westgate ME** (1991a) Maize kernel set at low water potential: II.  
844 Sensitivity to reduced assimilates at pollination. *Crop Sci* 31: 1196–1203

845 **Schussler JR, Westgate ME** (1991b) Maize kernel set at low water potential: I.  
846 sensitivity to reduced assimilates during early kernel growth. *Crop Sci* 31: 1189–  
847 1195

848 **Takagi H, Ishiga Y, Watanabe S, Konishi T, Egusa M, Akiyoshi N, Matsuura T,**  
849 **Mori IC, Hirayama T, Kaminaka H, Shimada H, Sakamoto A** (2016) .Allantoin, a  
850 stress-related purine metabolite, can activate jasmonate signaling in a MYC2-  
851 regulated and abscisic acid-dependent manner. *J Exp Bot* 67: 2519-2532

852 **Trapnell C, Pachter, Salzberg SL** (2009) TopHat: discovering splice junctions with  
853 RNA-Seq. *Bioinformatics* 25(9):1105-1111

854 **Tsai AY, Gazzarini S** (2014) Trehalose-6-phosphate and SnRK1 kinases in plant  
855 development and signaling: the emerging picture. *Frontiers in Plant Science* 119:  
856 doi: 10.3389/fpls.2014.00119

857 **Virlouver L, Jacquemot M-P, Gernetes D, Corti H, Bouton S, Gilard F, Valot B,**  
858 **Trouverie J, Tcherkez G, Falque M, Damerval C, Rogowsky P, Perez P, Noctor**  
859 **G, Zivy M, Coursol S** (2011) The ZmASR1 protein influences branched-chain amino  
860 acid biosynthesis and maintains kernel yield in maize under water-limited conditions.  
861 *Plant Physiology* 157, 917-936

862 **Wu D, Lim E, Vaillant F, Asselin-Labat ML, Visvader JE, Smyth GK** (2010)  
863 ROAST: rotation gene set tests for complex microarray experiments. *Bioinformatics*  
864 26, 2176–2182

865 **Yadav UP, Ivakov A, Feil R, Duan GY, Walther D, Giavalisco P, Piques M,**  
866 **Carillo P, Hubberten HM, Stitt M, Lunn JE** (2014) The sucrose-trehalose 6-

867 phosphate nexus: specificity and mechanisms of sucrose signalling by Tre6P. *J Exp*  
868 *Bot* 65: 1051-1068

869 **Zhang Y, Primavesi LF, Jhurreea D, Andralojc PJ, Mitchell RAC, Powers SJ,**  
870 **Schluepmann H, Delatte T, Wingler A, Paul MJ** (2009) Inhibition of Snf1-related  
871 protein kinase (SnRK1) activity and regulation of metabolic pathways by trehalose 6-  
872 phosphate. *Plant Physiology* 149: 1860-1871

873 **Zinselmeier C, Westgate ME, Schussler JR, Jones RJ** (1995a) Low water  
874 potential disrupts carbohydrate metabolism in maize (*Zea mays* L.) ovaries. *Plant*  
875 *Physiol* 107: 385–391

876 **Zinselmeier C, Lauer MJ, Boyer JS** (1995b) Reversing drought-induced losses in  
877 grain yield: sucrose maintains embryo growth in maize. *Crop Sci* 35: 1390–1400

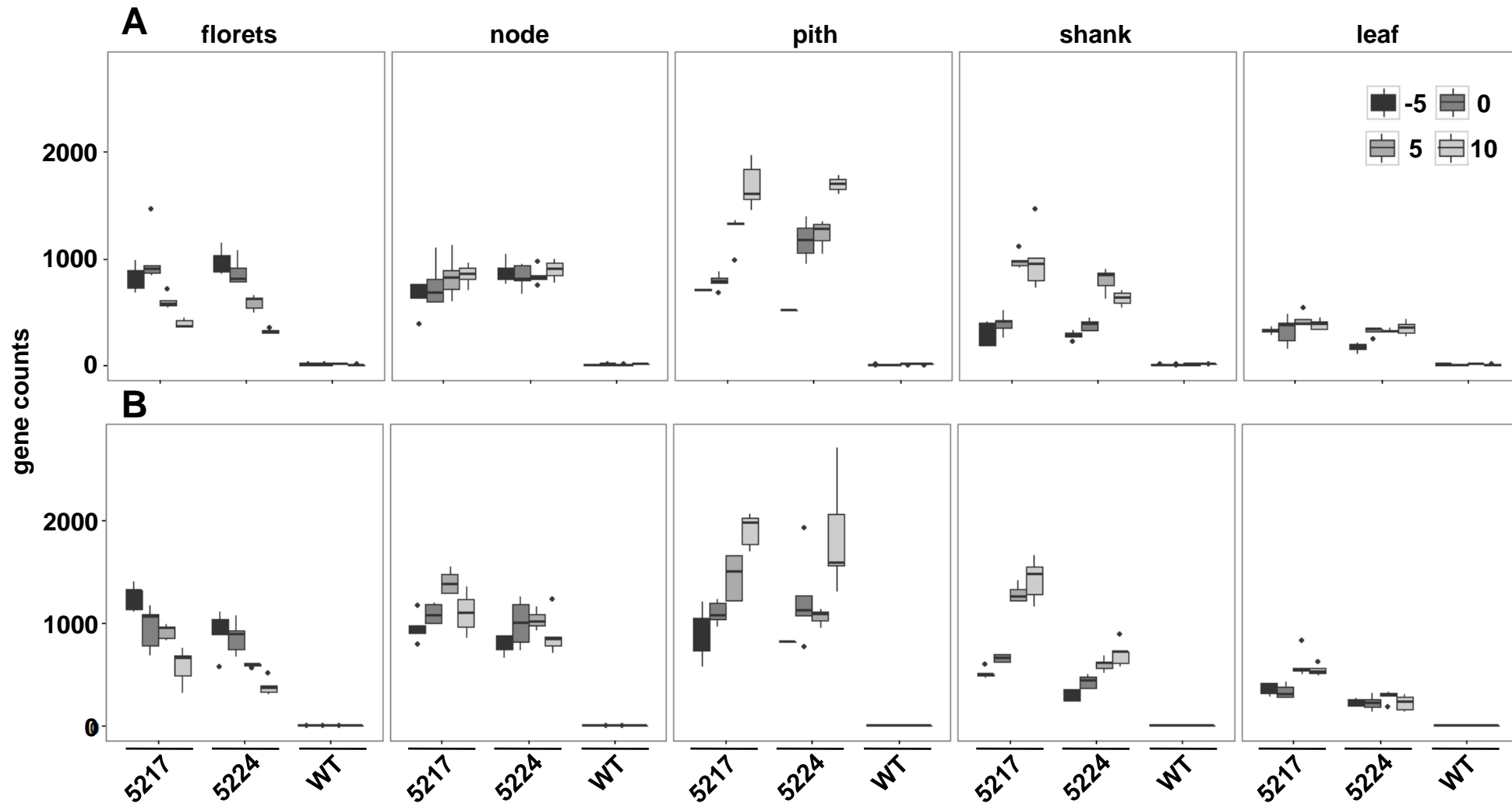


**Figure 1.** *OSMADS6: TPP1* expression in various maize tissues during early reproductive development. Data are from **(A)** unstressed and **(B)** drought stressed plants. Normalized gene count data are plotted for each transgenic event (5217 or 5224) and the wild-type (WT). The horizontal line in the each box indicates the mean. Vertical lines indicate the range for each sample. The time points are 5 days before pollination (-5), day of pollination (0), 5 days after pollination (5), and 10 days after pollination (10). Data are the mean +/- SD of 5 biological replicates

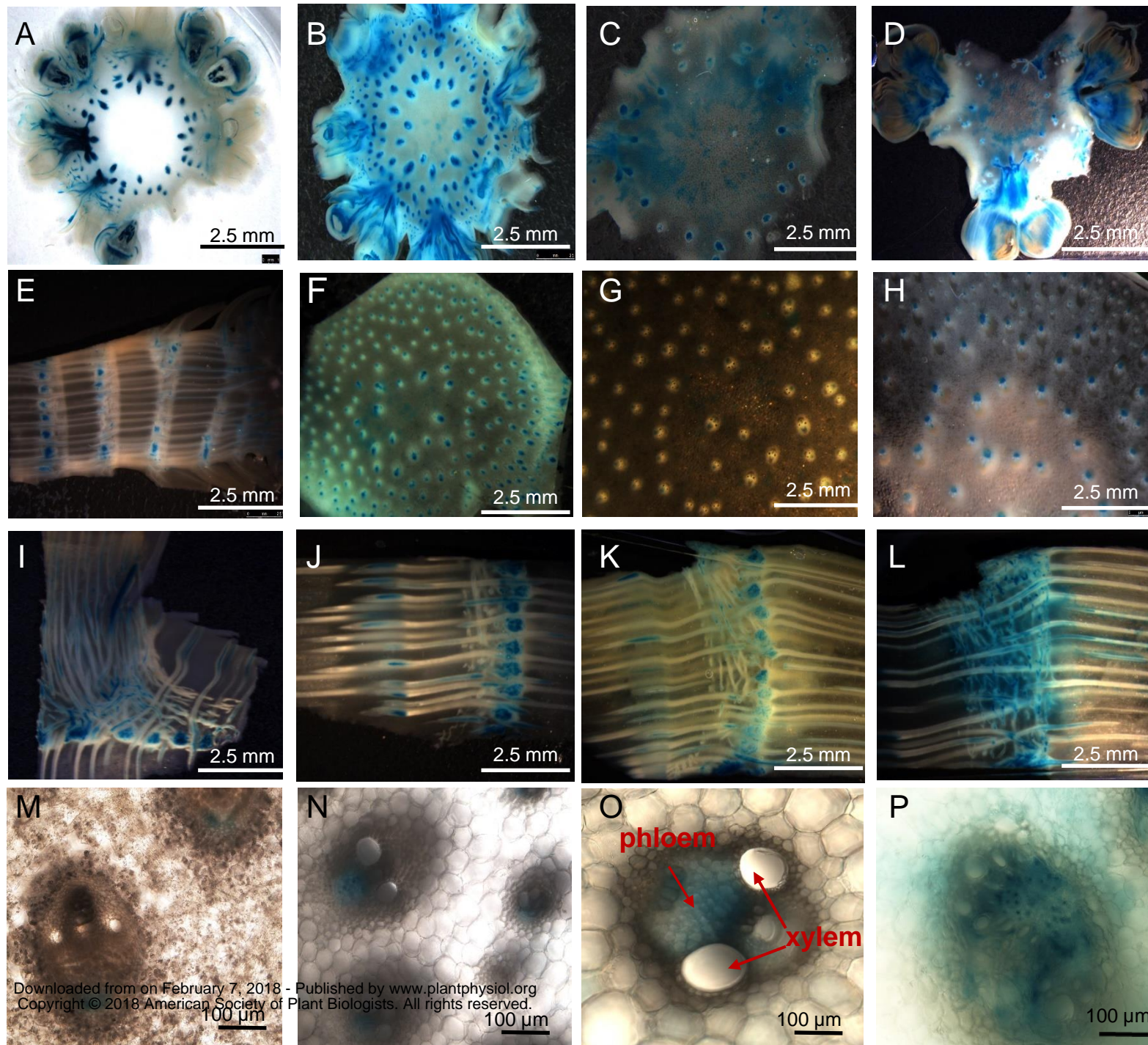


**Figure 2.** Histochemical localization of  $\beta$ -glucuronidase activity produced by the OsMads6-GUS reporter gene in unstressed maize during early reproductive development. Samples were collected from (A-D) ear spikelets, (E-H) shank, (I-L) node, (M-N) shank at high magnification, (O) node at high magnification, (P) pith at high magnification. Samples were collected at 5 days before pollination (A, E, I, M), day of pollination (B, F, J, N), 5 days after pollination (C, G, K, O) and 10 days after pollination (D, H, L, P). Samples were incubated in the histochemical reagent and cleared as described in the Methods. Xylem and phloem cells are indicated by the red arrows.

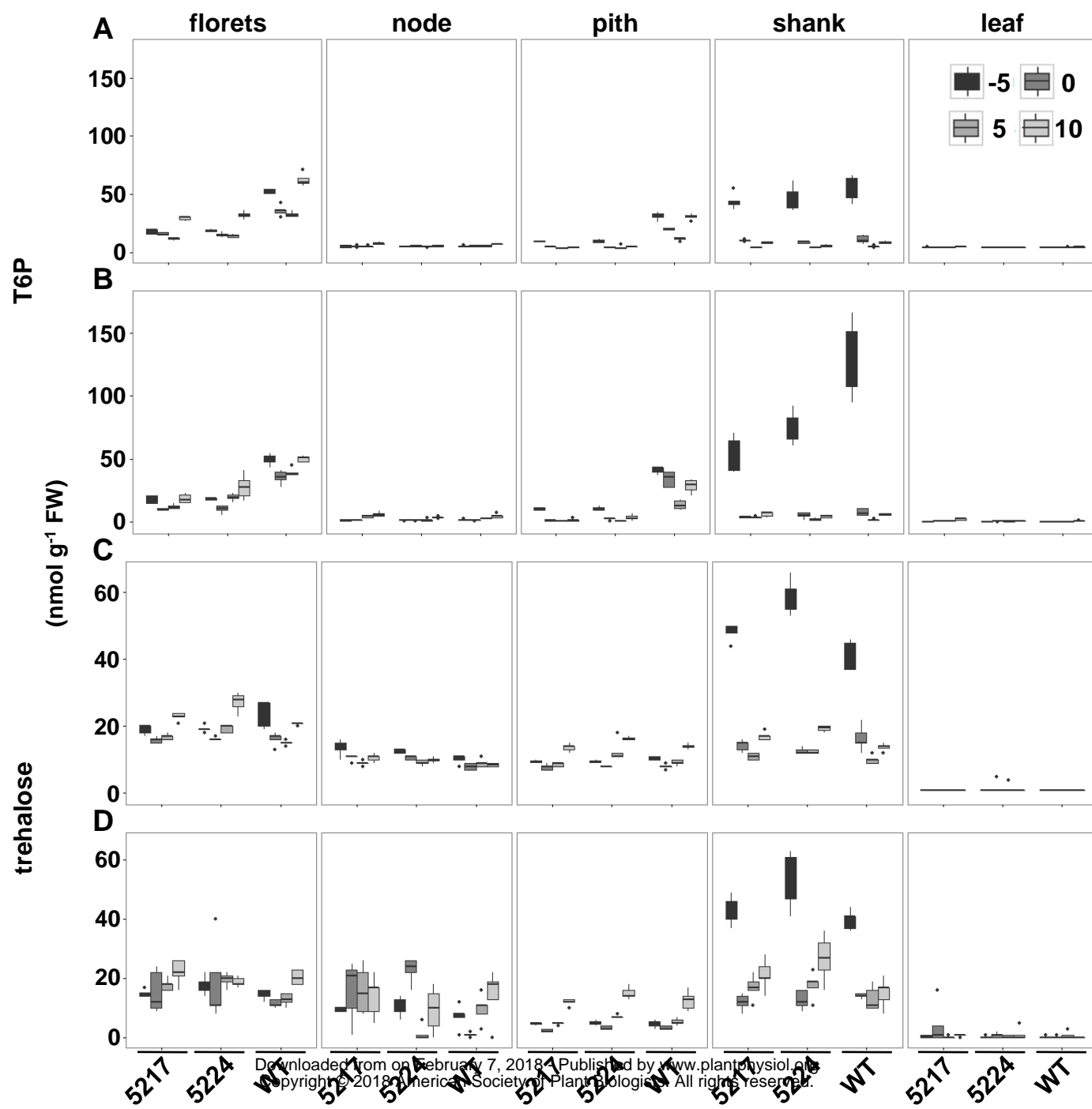


**Figure 3.** Effect of the *OSMADS6: TPP1* on T6P and trehalose in various tissues during early reproductive development comparing lines 5217, 5224 with wild type (WT). Samples were collected from **(A, C)** unstressed and **(B, D)** drought stressed plants. The time points are as in Figure 1. Data are the mean ± SD (n=4).

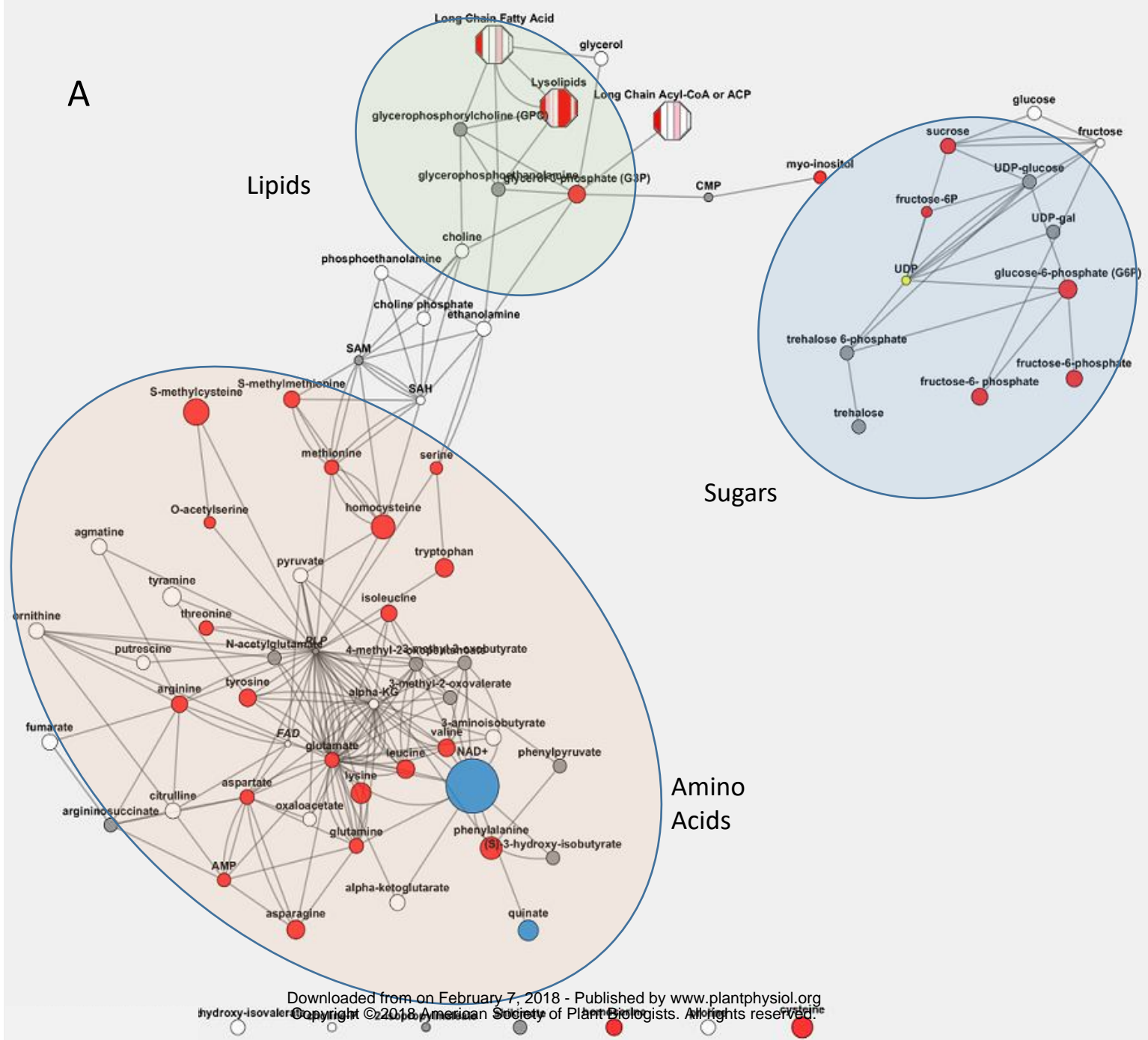


**Figure 4.** Screen shot from Metabosync showing change in metabolite abundance in response to *OSMADS6: TPP1*. Representative contrasts of transgenic event 5224 compared to wild type grown in unstressed conditions to show full extent of metabolite changes. **A.** Floret tissue at day of pollination. **B.** Pith tissue 5 days after pollination. Biochemicals shown are key metabolites in aromatic amino acid metabolism, glutamate family amino acid synthesis, phospholipid metabolism, sucrose metabolism, aspartate family amino acid synthesis, arginine biosynthesis, BCAA metabolism, trehalose biosynthesis and nitrogen metabolism. Circles represent metabolites as labeled. The size of the circle indicates statistical significance of difference of mean values from Welch's T-tests. Blue indicates fold change (ratio of mean value from all replicates in samples of transgenic event/ wild type) of less than one and red indicates fold change of greater than one.



B

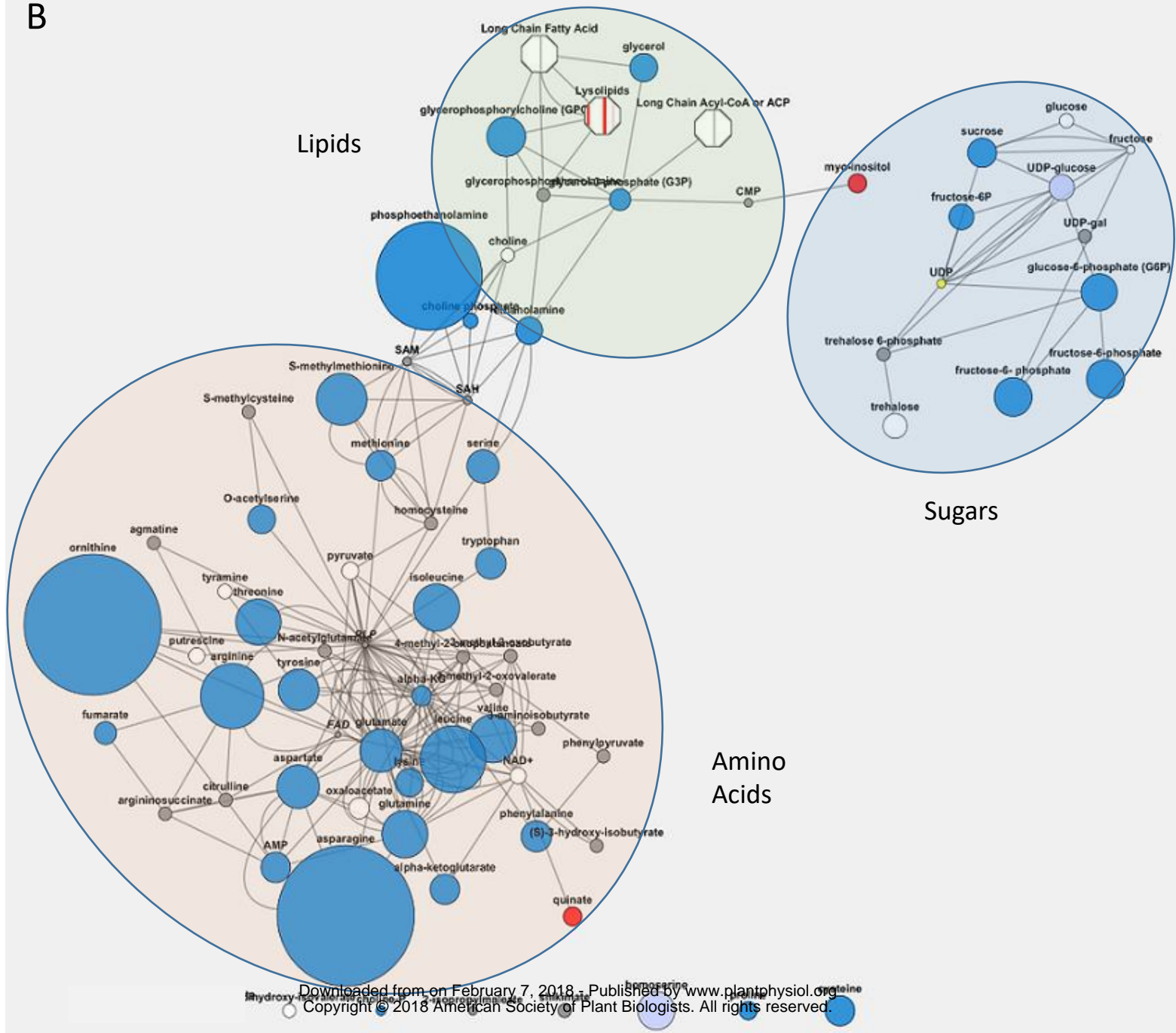


**Figure 4.** Screen shot from Metabosync showing change in metabolite abundance in response to *OSMADS6: TPP1*. Representative contrasts of transgenic event 5224 compared to wild type grown in unstressed conditions to show full extent of metabolite changes. **A.** Floret tissue at day of pollination. **B.** Pith tissue 5 days after pollination. Biochemicals shown are key metabolites in aromatic amino acid metabolism, glutamate family amino acid synthesis, phospholipid metabolism, sucrose metabolism, aspartate family amino acid synthesis, arginine biosynthesis, BCAA metabolism, trehalose biosynthesis and nitrogen metabolism. Circles represent metabolites as labeled. The size of the circle indicates statistical significance of difference of mean values from Welch's T-tests. Blue indicates fold change (ratio of mean value from all replicates in samples of transgenic event/ wild type) of less than one and red indicates fold change of greater than one.

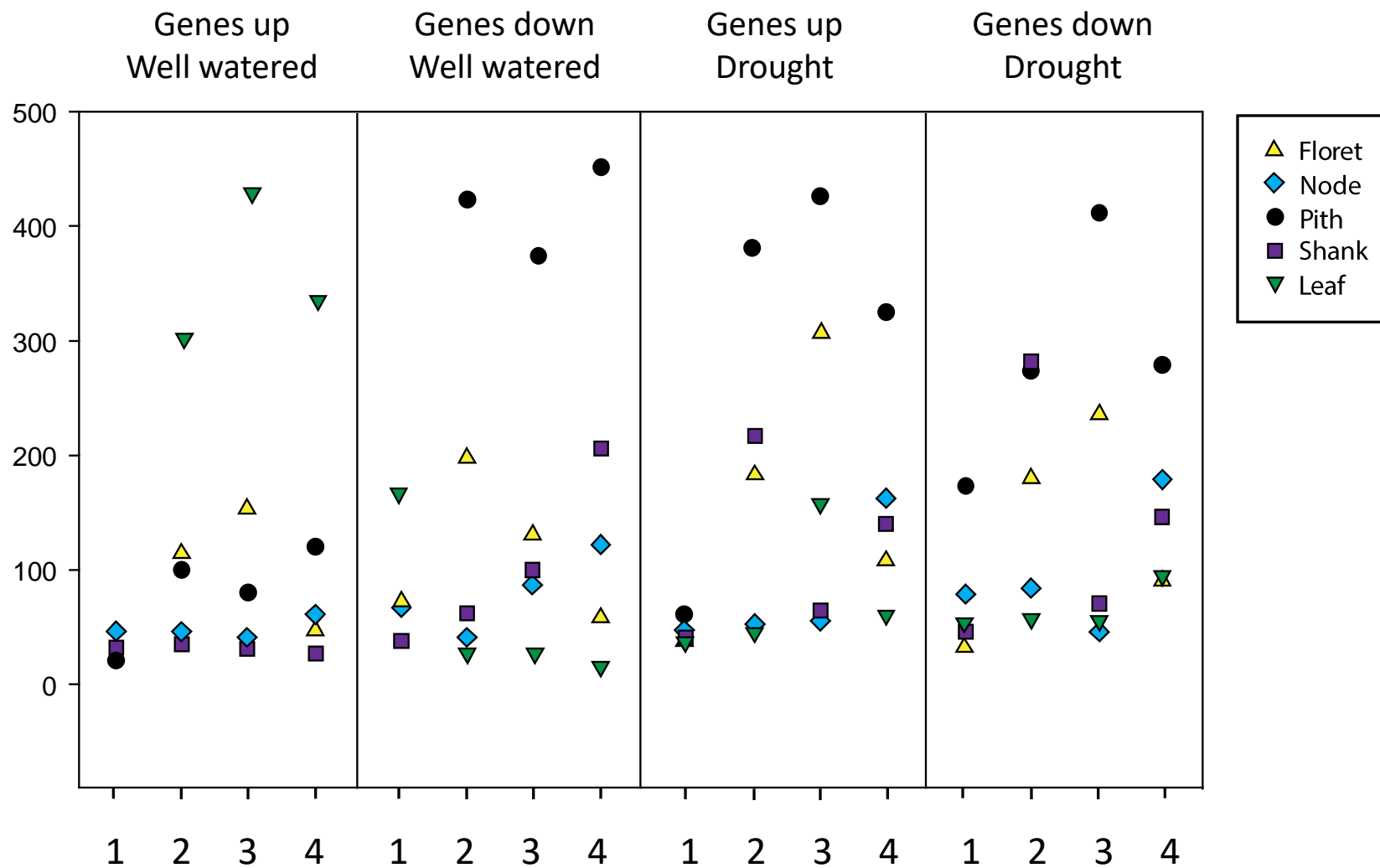


**Figure 5.** Genes significantly upregulated or down regulated in different tissues in both *OSMADS6: TPP1* transgenic lines compared to wild type in well-watered conditions and under drought. The time points are 5 days before pollination (1), day of pollination (2), 5 days after pollination (3), and 10 days after pollination (4).

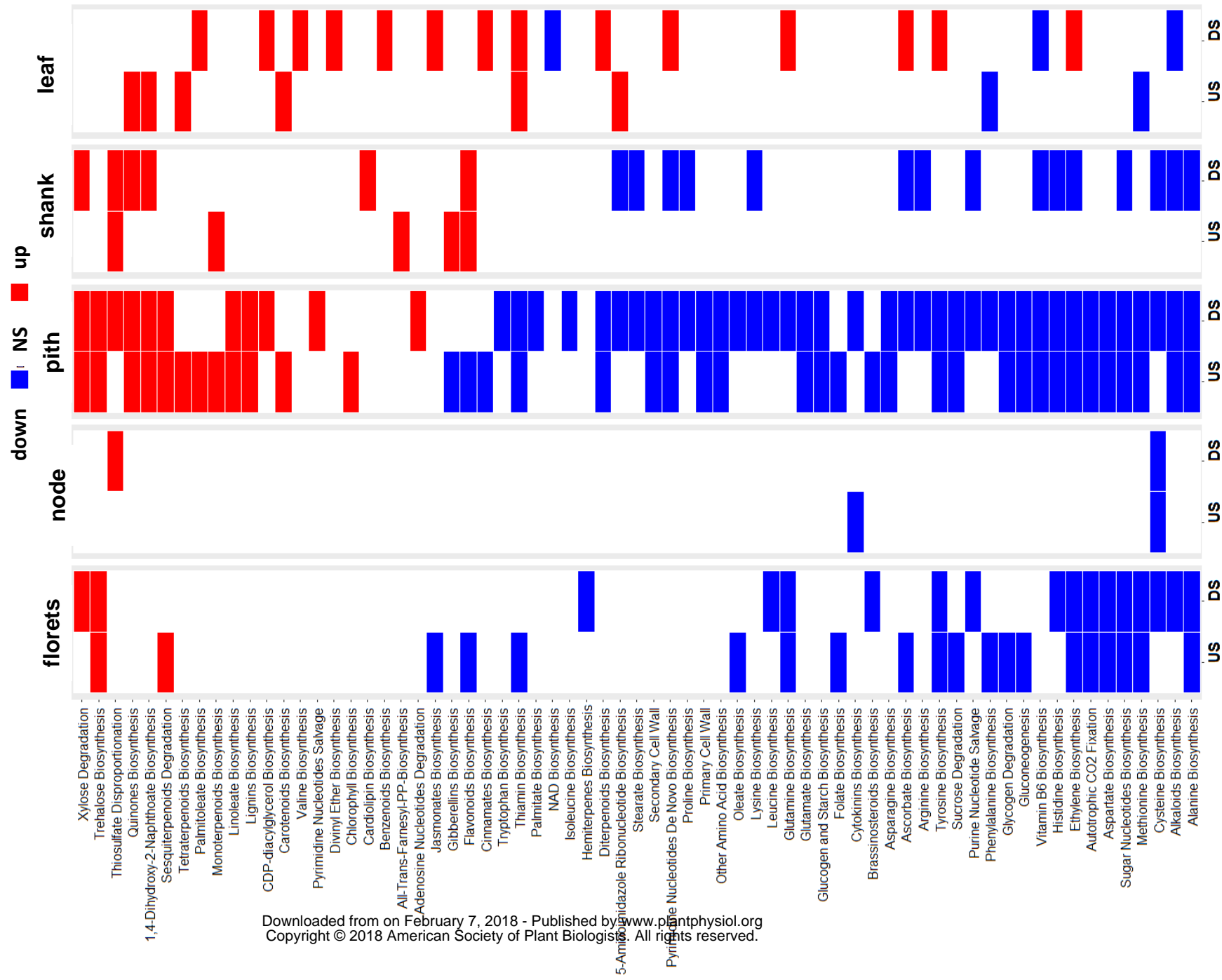
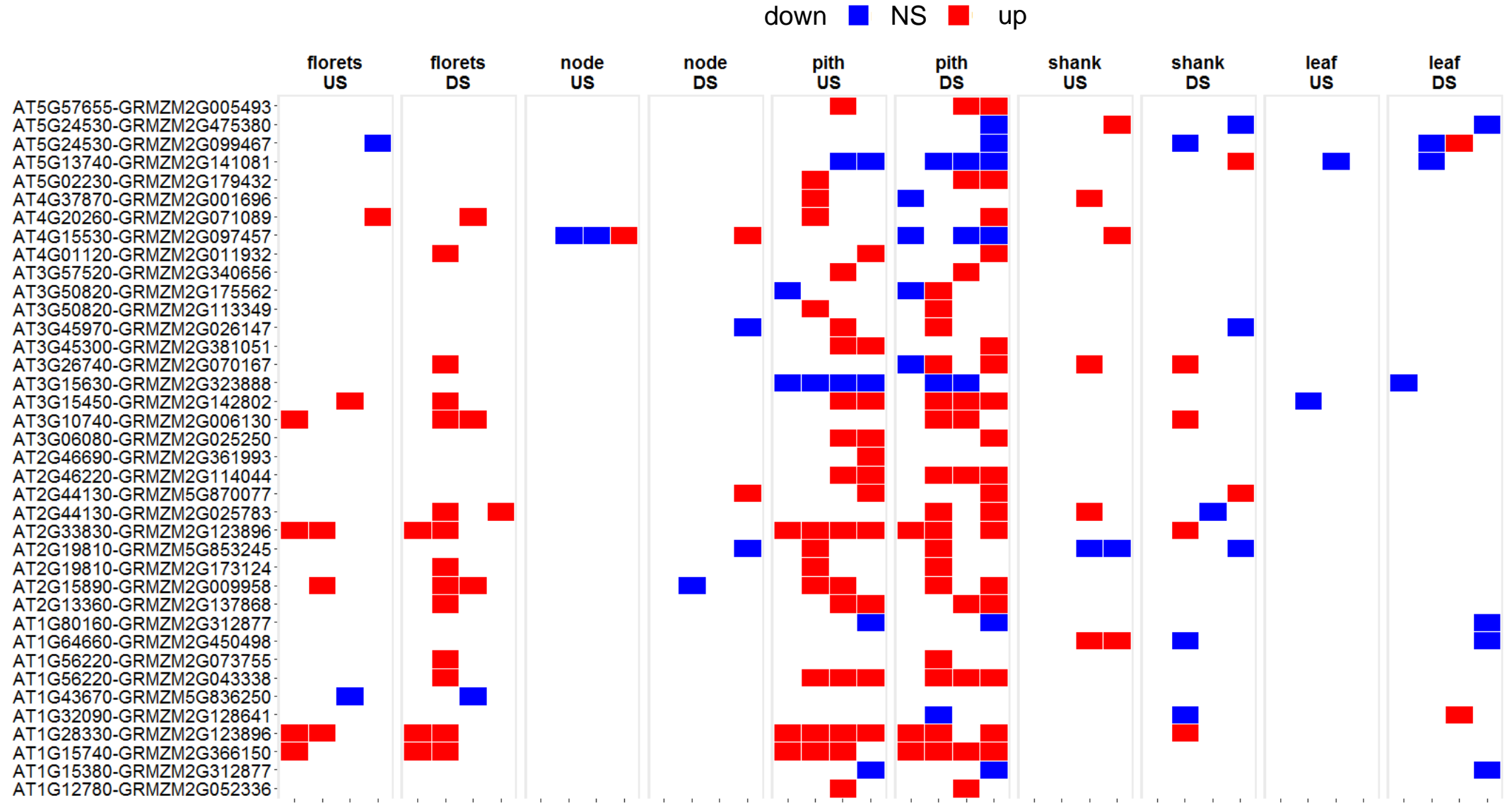


**Figure 6.** *OSMADS6*: *TPP1* effect on biochemical pathways in maize. Transcript profiling data from both the 5217 and 5224 events were compared to wildtype to identify significantly perturbed biochemical pathways. A white cell indicates pathways that were not affected and a dark cell indicates pathways that were significantly affected by the transgene. The data are from unstressed and drought stressed plants. Results from the four time points were condensed by only reporting pathways significantly affected in at least two time points.

**Figure 7.** Heat map showing the *OSMADS6:TPP1* effect on SnRK1 regulated genes.

Transcript profiling data from both the 5217 and 5224 events compared to wildtype. The *OsMads6-Tpp1* effect on maize orthologs of Arabidopsis/wheat genes shown to be (A) induced by SnRK1 using differential expression analysis. The data represent the indicated tissues harvested from unstressed (US) or drought stressed (DS) plants. Red indicates up-regulation and blue indicates down-regulation relative to wildtype (A188). White indicates no significant (NS). Time points shown on the x-axis are 1, 5 days before pollination; 2, Day of pollination; 3, 5 days after pollination; 4, 10 days after pollination.



down ■ NS ■ up

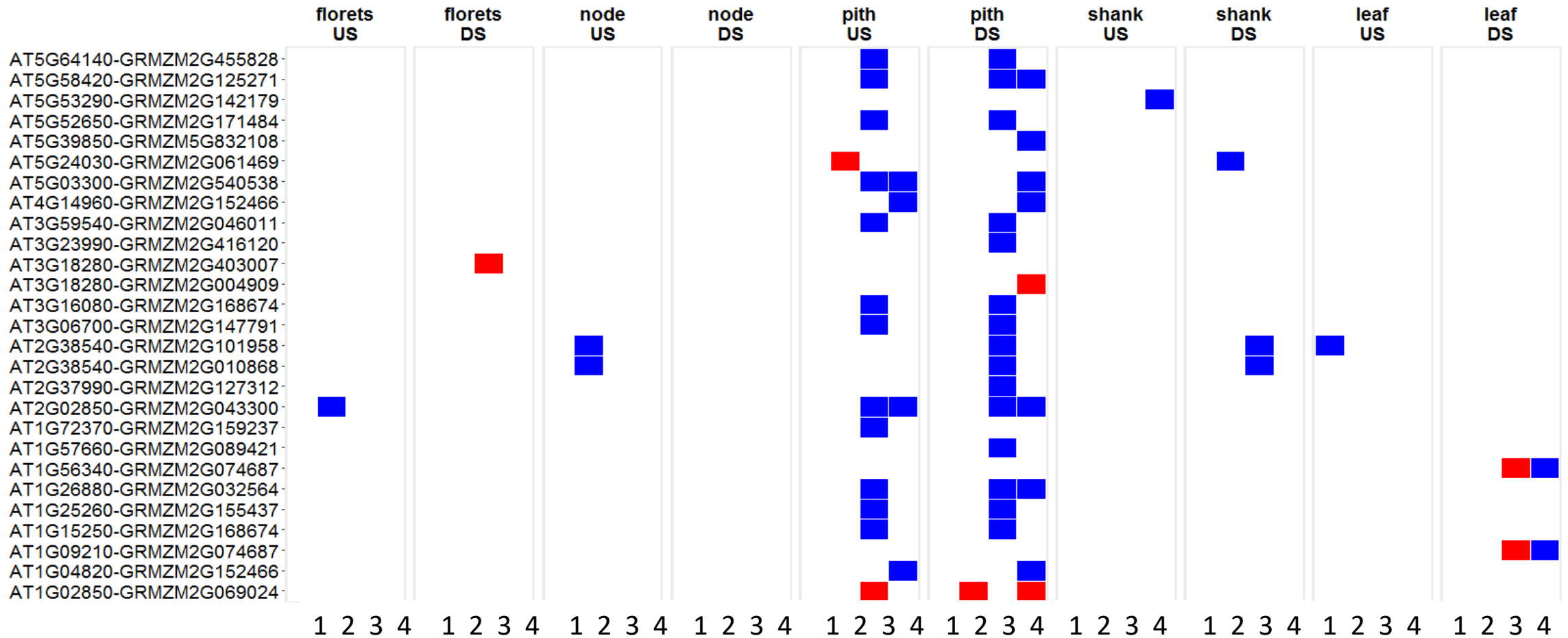


**Figure 7.** Heat map showing the *OSMADS6: TPP1* effect on SnRK1 regulated genes. Transcript profiling data from both the 5217 and 5224 events compared to wildtype. The *OsMads6-Tpp1* effect on maize orthologs of Arabidopsis/wheat genes shown to be **(B)** induced by SnRK1 using differential expression analysis. The data represent the indicated tissues harvested from unstressed (US) or drought stressed (DS) plants. Red indicates up-regulation and blue indicates down-regulation relative to wildtype (A188). White indicates no significant (NS). Time points shown on the x-axis are 1, 5 days before pollination; 2, Day of pollination; 3, 5 days after pollination; 4, 10 days after pollination.

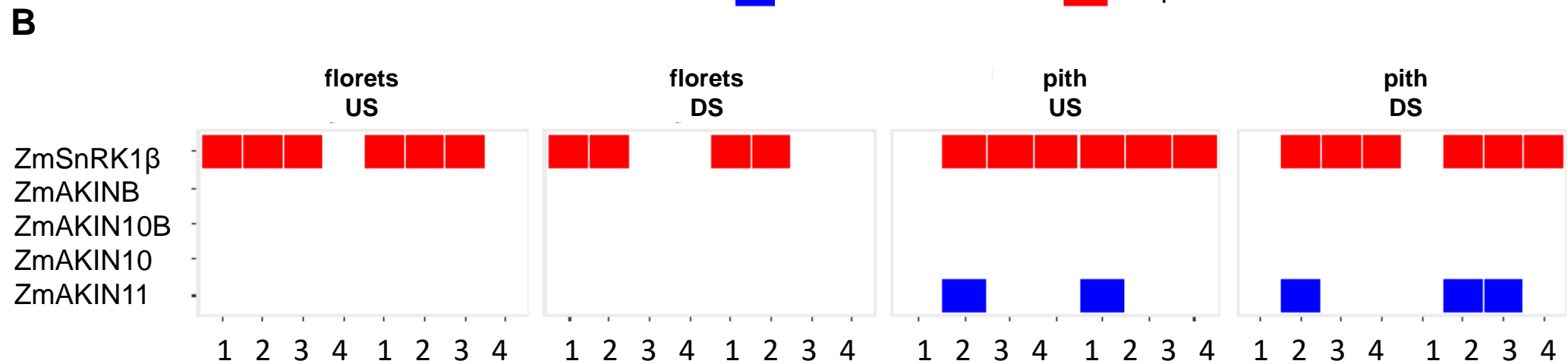
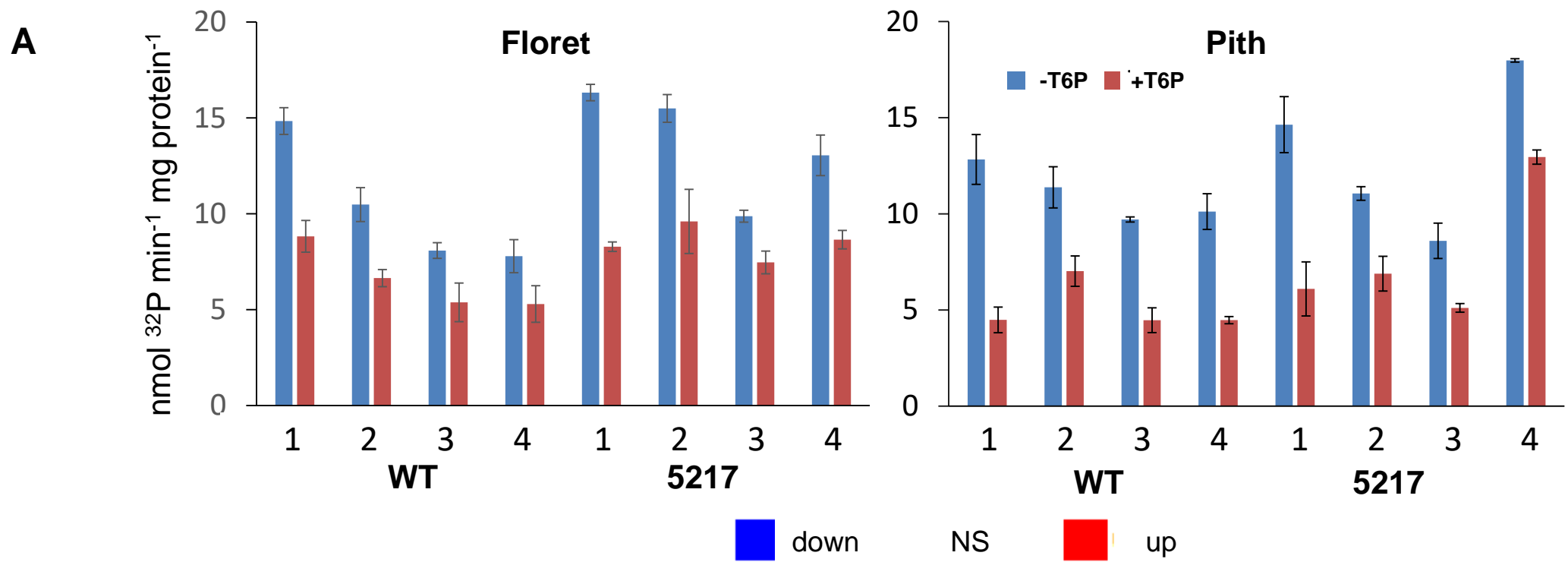


**Figure 8.** *OSMADS6: TPP1* effect on SnRK1 activity. Pith and floret tissues were examined for (A) Extractable SnRK1 activity (line 5217) and (B) effect on maize orthologs of Arabidopsis genes that encode SnRK1 subunits (lines 5217, 5224). SnRK1 activity was assayed in the presence and absence of 1 mM T6P. Data are the mean  $\pm$  SD ( $n = 3$ ). The maize genes are ZmSNRK1 $\beta$ , GRMZM2G025459; ZmAKINB, GRMZM2G138814; ZmAKIN10B, GRMZM2G077278; ZmAKIN10, GRMZM2G077278; ZmAKIN11, GRMZM2G107867. The time points are 5 days before pollination (1), day of pollination (2), 5 days after pollination (3), and 10 days after pollination (4).

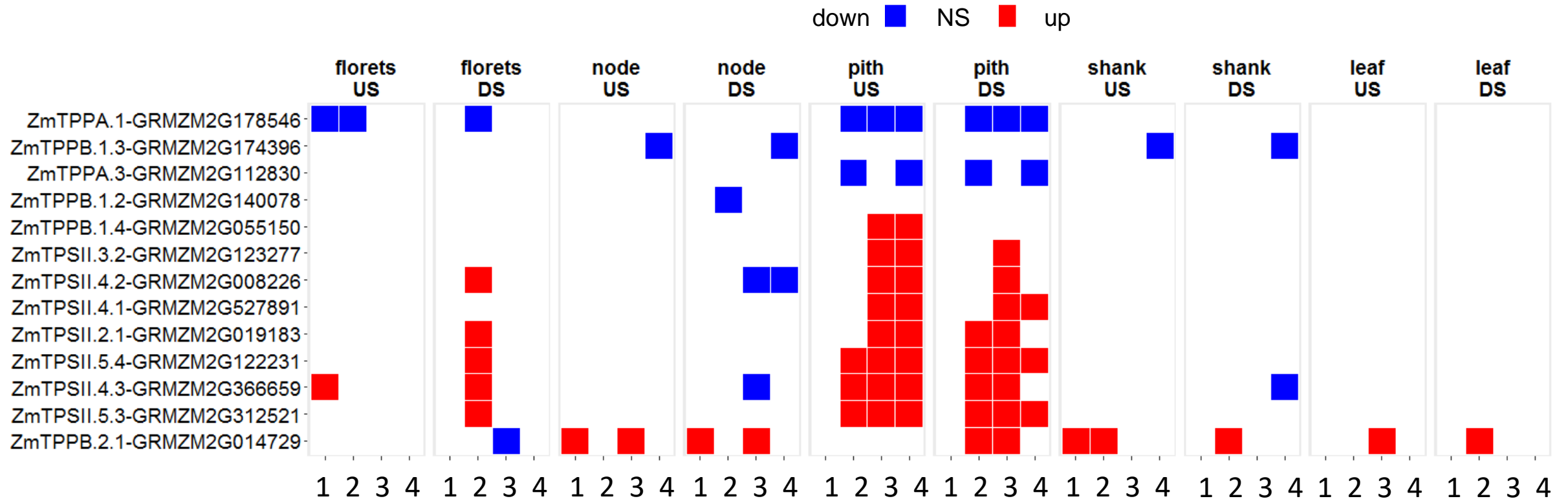


**Figure 9.** *OSMADS6*: *TPP1* effect on trehalose metabolism gene expression, trehalose-6-phosphate synthase (TPS) and trehalose-6-phosphate phosphatase (TPP) gene family members evaluated using differential expression analysis. Only genes that changed significantly in both events in the same direction temporally and spatially are reported. The time points are 5 days before pollination (1), day of pollination (2), 5 days after pollination (3) and 10 days after pollination (4).

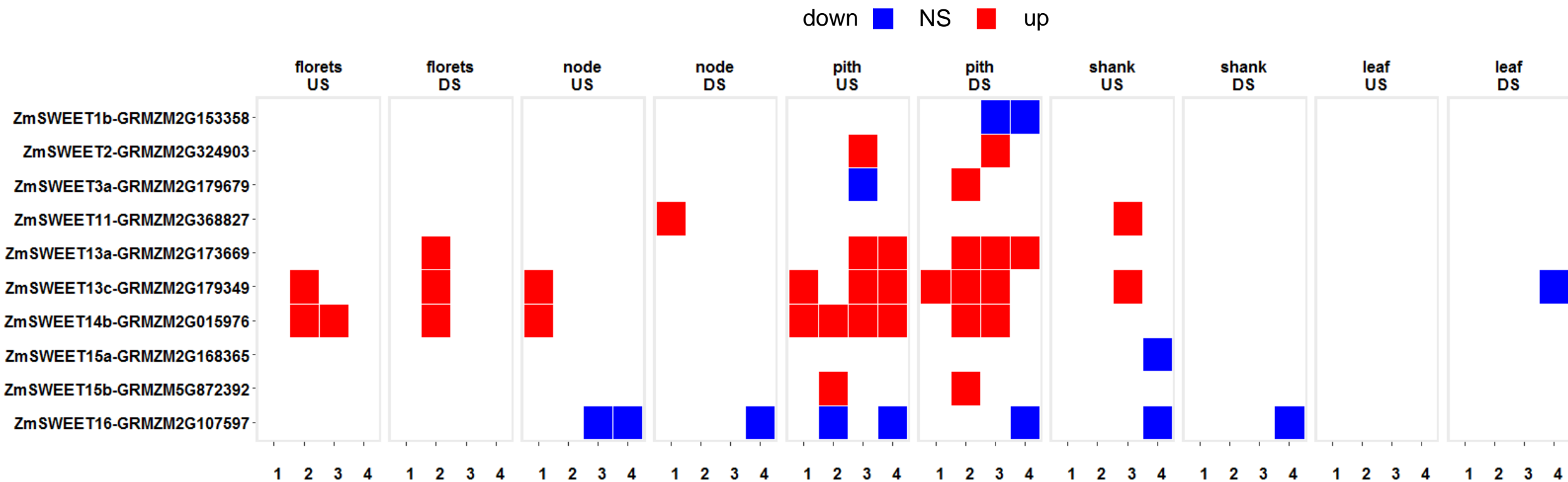


**Figure 10.** Heat map showing the effect of *OSMADS6: TPP1* on SWEET genes. Heat maps represent differential expression analysis between wild type and transgenic lines 5217 and 5224. Only genes that changed significantly in both events in the same direction temporally and spatially are reported. The time points are 5 days before pollination (1), day of pollination (2), 5 days after pollination (3) and 10 days after pollination (4).



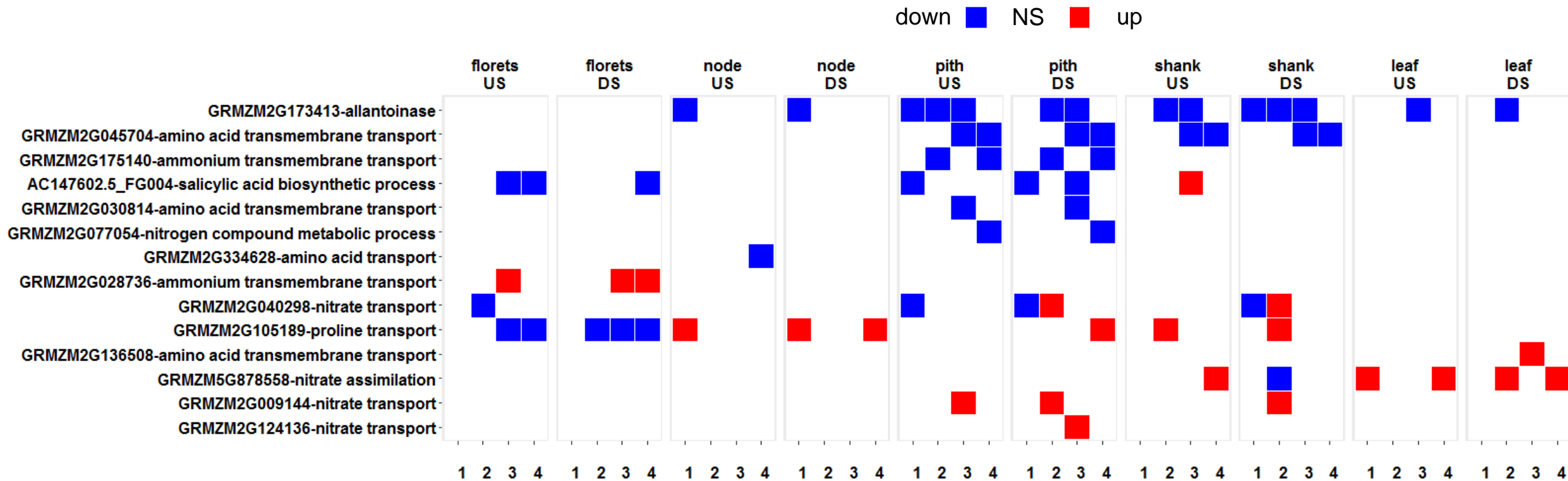


**Figure 11.** Heat map of differential expression of allantoinase and nitrogen metabolism genes in transgenic lines compared to wild type. Only genes that changed significantly in both events in the same direction are reported. The time points are 5 days before pollination (1), day of pollination (2), 5 days after pollination (3) and 10 days after pollination (4).

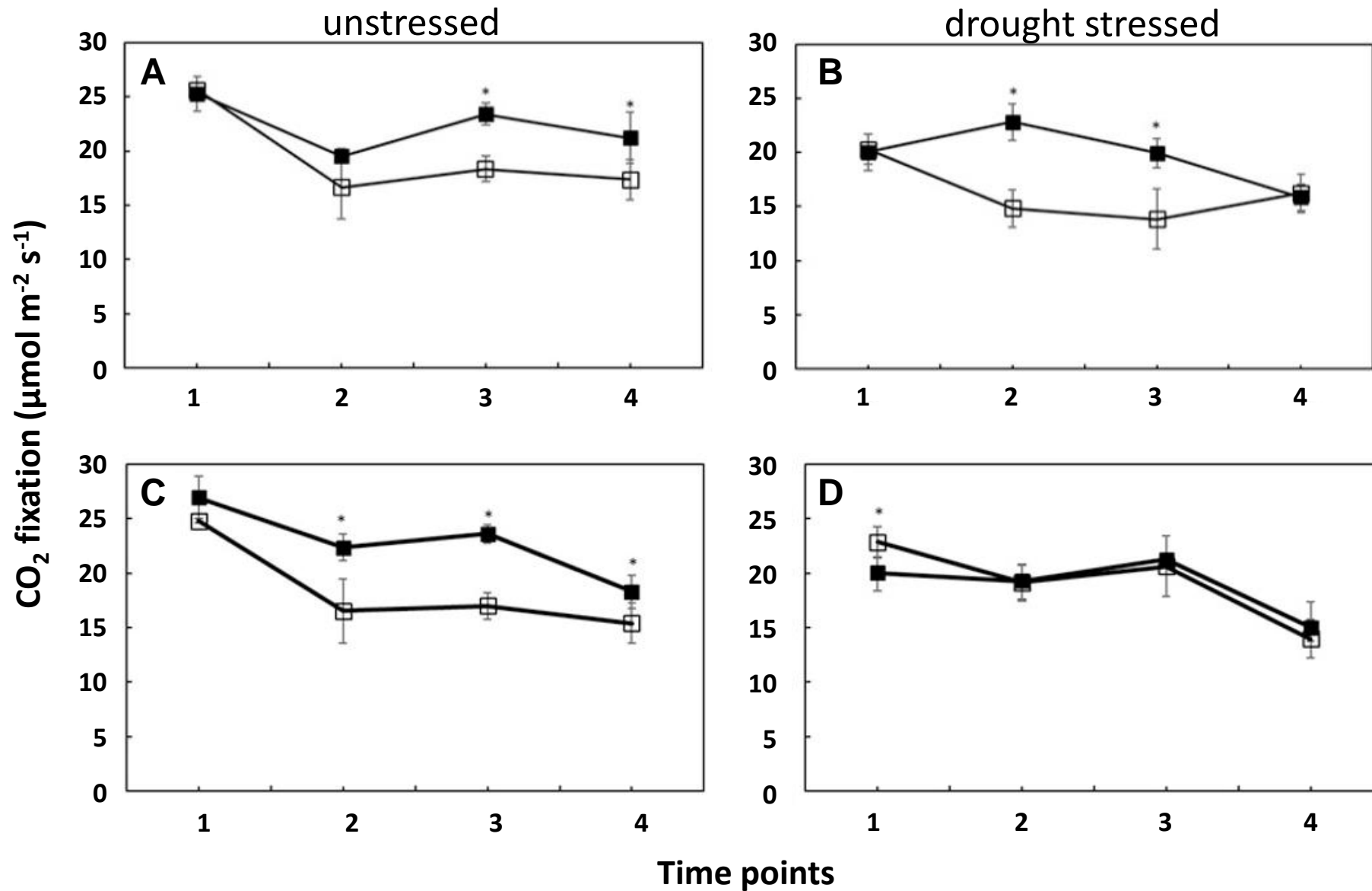


**Figure 12.** The effect of *OSMADS6: TPP1* on photoassimilation in leaf during reproductive development. The CO<sub>2</sub> uptake rate was measured using an infrared gas analyzer in (A, B) the ear leaf and (C, D) the leaf above the ear during the two week reproductive period (need better context). Unstressed (A, C) and drought stressed (B, D). Wildtype □ and event 5224 ■ plants were evaluated. The time points are 5 days before pollination (1), day of pollination (2), 5 days after pollination (3) and 10 days after pollination (4). Data are the mean ± SD (n = 4). \* denotes statistical significance at p < 0.05.

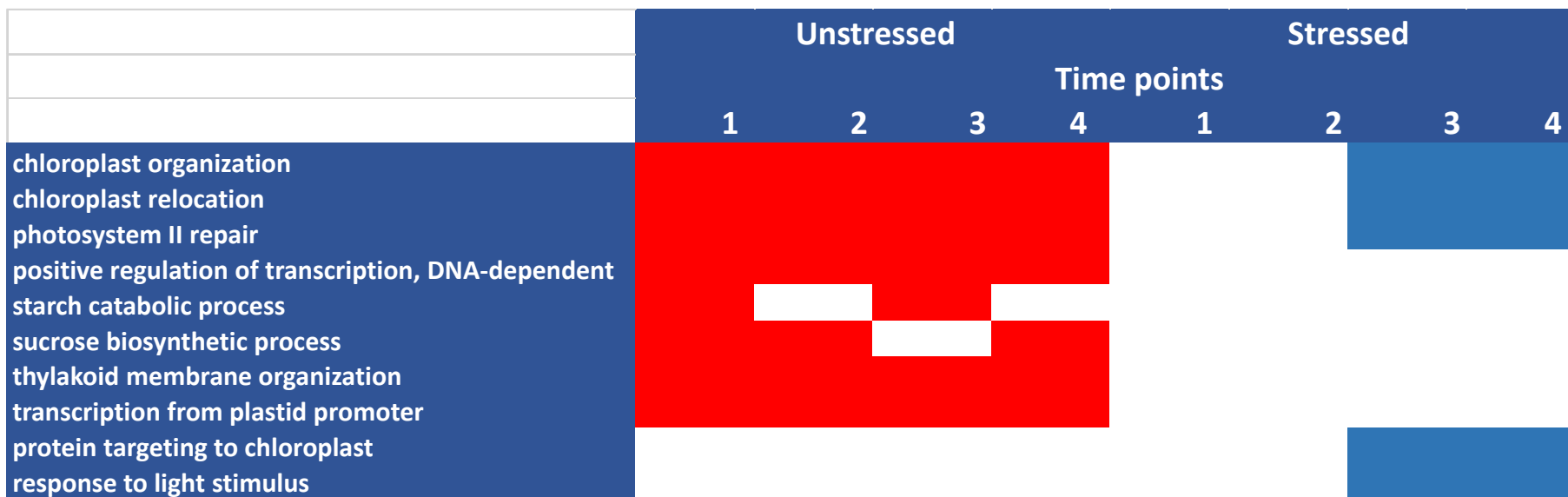


**Figure 13.** *OSMADS6: TPP1* affected genes with gene ontology terms associated with photosynthesis. Transcript profiling data from both the 5217 and 5224 events were compared to wildtype to identify significantly perturbed GO terms. A white cell indicates pathways that were not affected and a dark cell indicates pathways that were significantly affected by the transgene. Only pathways significantly enriched in both events are shown. The time points are 5 days before pollination (1), day of pollination (2), 5 days after pollination (3) and 10 days after pollination (4).

## Parsed Citations

**Baena-Gonzalez E, Rolland F, Thevelein JM, Sheen J (2007) A central integrator of transcription networks in plant stress and energy signalling. *Nature* 448, 938-942**

Pubmed: [Author and Title](#)

CrossRef: [Author and Title](#)

Google Scholar: [Author Only](#) [Title Only](#) [Author and Title](#)

**Baena-Gonzalez E, Hanson J (2017) Shaping plant development through the SnRK-TOR metabolic regulators. *Current Opinion in Plant Biology* 35, 152-157**

Pubmed: [Author and Title](#)

CrossRef: [Author and Title](#)

Google Scholar: [Author Only](#) [Title Only](#) [Author and Title](#)

**Bezruczyk M, Hartwig T, Horshman M, Nian Char S, Yang J, Yang B, Frommer WB, Sosso D (2017) Impaired phloem loading in genome-edited triple knock-out mutants of SWEET13 sucrose transporters. *Biorxiv* doi.org/10.1101/197921**

Pubmed: [Author and Title](#)

CrossRef: [Author and Title](#)

Google Scholar: [Author Only](#) [Title Only](#) [Author and Title](#)

**Boyer JS, McLaughlin JE (2007) Functional reversion to identify controlling genes in multigenic responses: analysis of floral abortion. *J Exp Bot* 58: 267-277**

Pubmed: [Author and Title](#)

CrossRef: [Author and Title](#)

Google Scholar: [Author Only](#) [Title Only](#) [Author and Title](#)

**Boyer JS, Westgate ME (2004) Grain yields with limited water. *J Exp Bot* 55: 385-2394**

Pubmed: [Author and Title](#)

CrossRef: [Author and Title](#)

Google Scholar: [Author Only](#) [Title Only](#) [Author and Title](#)

**Boyer J, Byrne P, Cassman K, Cooper M, Delmer D, Greene T, et al. (2013) The US drought of 2012 in perspective: A call to action. *Global Food Security* 2:139-43**

Pubmed: [Author and Title](#)

CrossRef: [Author and Title](#)

Google Scholar: [Author Only](#) [Title Only](#) [Author and Title](#)

**Braun DM, Wang L, Ruan Y-L (2014) Understanding and manipulating sucrose phloem loading, unloading, metabolism, and signalling to enhance crop yield and food security. *Journal of Experimental Botany* 65, 1713-1735**

Pubmed: [Author and Title](#)

CrossRef: [Author and Title](#)

Google Scholar: [Author Only](#) [Title Only](#) [Author and Title](#)

**Brychkova G, Alikulov Z, Fluhr R, Sagi M (2008) A critical role for ureides in dark and senescence-induced purine remobilization is unmasked in the *Atxdh1* Arabidopsis mutant. *Plant Journal* 54: 496-509**

Pubmed: [Author and Title](#)

CrossRef: [Author and Title](#)

Google Scholar: [Author Only](#) [Title Only](#) [Author and Title](#)

**Chen THH, Murata N (2002) Enhancement of tolerance of abiotic stress by metabolic engineering of betaines and other compatible solutes. *Current Opinion in Plant Biology* 5, 250-257**

Pubmed: [Author and Title](#)

CrossRef: [Author and Title](#)

Google Scholar: [Author Only](#) [Title Only](#) [Author and Title](#)

**Chen LQ, Hou BH, Lalonde S, Takanaga H, Hartung ML, Qu XQ, et al. (2010) Sugar transporters for intercellular exchange and nutrition of Pathogens. *Nature* 25: 527-532**

Pubmed: [Author and Title](#)

CrossRef: [Author and Title](#)

Google Scholar: [Author Only](#) [Title Only](#) [Author and Title](#)

**Collier, R and Tegeder M (2012) Soybean ureide transporters play a critical role in nodule development, function and nitrogen export. *Plant J* 72: 355-367**

Pubmed: [Author and Title](#)

CrossRef: [Author and Title](#)

Google Scholar: [Author Only](#) [Title Only](#) [Author and Title](#)

**Cortina C, Culiáñez-Macià FA (2005) Tomato abiotic stress enhanced tolerance by trehalose biosynthesis. *Plant Sci* 169: 75-82**

Pubmed: [Author and Title](#)

CrossRef: [Author and Title](#)

Google Scholar: [Author Only](#) [Title Only](#) [Author and Title](#)

**Delatte TL, Sedijani P, Kondou Y, Matsui M, de Jong GJ, Somsen GW, Wiese-Klinkenberg A, Primavesi LF, Paul MJ, Schlupepmann H (2011) Growth arrest by trehalose-6-phosphate: an astonishing case of primary metabolite control over growth by way of the SnRK1**

Downloaded from on February 7, 2018 - Published by www.plantphysiol.org

Copyright © 2018 American Society of Plant Biologists. All rights reserved.

**signaling pathway. Plant Physiology 157: 160-174**

Pubmed: [Author and Title](#)

CrossRef: [Author and Title](#)

Google Scholar: [Author Only](#) [Title Only](#) [Author and Title](#)

**Durand M, Mainson D, Porcheron B, Maurousset L, Lemoine R, Portau N (2017) Carbon source-sink relationship in Arabidopsis thaliana: the role of sucrose transporters. Planta doi.org/10.1007/s00425-017-2807-4**

Pubmed: [Author and Title](#)

CrossRef: [Author and Title](#)

Google Scholar: [Author Only](#) [Title Only](#) [Author and Title](#)

**Figuroa CM, Feil R1, Ishihara H, Watanabe M, Kölling K, Krause U, Höhne M, Encke B, Plaxton WC, Zeeman SC, Li Z, Schulze WX, Hoefgen R, Stitt M, Lunn JE (2016) Trehalose 6-phosphate coordinates organic and amino acid metabolism with carbon availability. Plant J 85: 410-423**

Pubmed: [Author and Title](#)

CrossRef: [Author and Title](#)

Google Scholar: [Author Only](#) [Title Only](#) [Author and Title](#)

**Habben JE, Bao X, Bate NJ, Debruin JL, Dolan D, Hasegawa D, et al. (2014) Transgenic alteration of ethylene biosynthesis increases grain yield in maize under field drought-stress conditions. Plant Biotechnol J 12: 685-93**

Pubmed: [Author and Title](#)

CrossRef: [Author and Title](#)

Google Scholar: [Author Only](#) [Title Only](#) [Author and Title](#)

**Henry C, Bledsoe SW, Siekman A, Kollman A, Waters BM, Feil R, Stitt M, Lagrimini LM (2014) The trehalose pathway in maize: conservation and gene regulation in response to the diurnal cycle and extended darkness. J Ex Bot 65: 5959-5973**

Pubmed: [Author and Title](#)

CrossRef: [Author and Title](#)

Google Scholar: [Author Only](#) [Title Only](#) [Author and Title](#)

**Kolbe A, Tiessen A, Schluempmann H, Paul MJ, Ulrich S, Geigenberger P (2005) Trehalose 6-phosphate regulates starch synthesis via post-translational activation of ADP-glucose pyrophosphorylase. Proceedings of the National Academy of Sciences USA 102, 11118-11123**

Pubmed: [Author and Title](#)

CrossRef: [Author and Title](#)

Google Scholar: [Author Only](#) [Title Only](#) [Author and Title](#)

**Langmead B, Trapnell C, Pop M, Salzberg SL (2009) Ultrafast and memory-efficient alignment of short DNA sequences to the human genome. Genome Biology 10: R25 DOI: 10.1186/gb-2009-10-3-r25**

Pubmed: [Author and Title](#)

CrossRef: [Author and Title](#)

Google Scholar: [Author Only](#) [Title Only](#) [Author and Title](#)

**Li L, Stoeckert J, Roos DS (2003) OrthoMCL: Identification of Ortholog Groups for Eukaryotic Genomes. Genome Research 13: 2178-2189**

Pubmed: [Author and Title](#)

CrossRef: [Author and Title](#)

Google Scholar: [Author Only](#) [Title Only](#) [Author and Title](#)

**Lunn JE, Feil R, Hendriks JH, Gibon Y, Morcuende R, Osuna D, Scheible WR, Carillo P, Hajirezaei MR, Stitt M (2006) Sugar-induced increases in trehalose 6-phosphate are correlated with redox activation of ADPglucose pyrophosphorylase and higher rates of starch synthesis in Arabidopsis thaliana. Biochem J 397: 139-148**

Pubmed: [Author and Title](#)

CrossRef: [Author and Title](#)

Google Scholar: [Author Only](#) [Title Only](#) [Author and Title](#)

**Martínez-Barajas E, Delatte T, Schluempmann H, de Jong GJ, Somsen GW, Nunes C, Primavesi LF, Coello P, Mitchell RAC, Paul MJ (2011) Wheat grain development is characterised by remarkable T6P accumulation pre-grain filling: tissue distribution and relationship to SNF1-related protein kinase1 activity. Plant Physiology 156: 373-381**

Pubmed: [Author and Title](#)

CrossRef: [Author and Title](#)

Google Scholar: [Author Only](#) [Title Only](#) [Author and Title](#)

**Martins MCM, Hejazi M, Fettke J, Steup M, Feil R, Krause U, Arrivault S, Vosloh D, Figuroa CM, Ivakov A, Yadav UP, Piques M, Metzner D, Stitt M, Lunn JE (2013) Feedback inhibition of starch degradation in arabidopsis leaves mediated by trehalose 6-phosphate. Plant Physiology 163: 1142-1163**

Pubmed: [Author and Title](#)

CrossRef: [Author and Title](#)

Google Scholar: [Author Only](#) [Title Only](#) [Author and Title](#)

**Nuccio ML, Wu J, Mowers R, Zhou H-P, Meghji M, Primavesi LF, et al. (2015) Expression of trehalose 6-phosphate phosphatase in maize ears improves yield in well-watered and drought conditions. Nature Biotechnol 33: 862-874**

Pubmed: [Author and Title](#)

CrossRef: [Author and Title](#)

Google Scholar: [Author Only](#) [Title Only](#) [Author and Title](#)

**Nunes C, O'Hara, Primavesi LF, Delatte TL, Schluempmann H, Somsen GW, et al., (2013a) The T6P/ SnRK1 signaling pathway primes growth recovery following relief of sink limitation. *Plant Physiol* 162: 1720-1732**

Pubmed: [Author and Title](#)

CrossRef: [Author and Title](#)

Google Scholar: [Author Only Title Only Author and Title](#)

**Nunes C, Primavesi LF, Patel MK, Martinez-Barajas E, Powers SJ, Sagar R, Fevereiro PS, Davis BG, Paul MJ (2013b) Inhibition of SnRK1 by metabolites: tissue-dependent effects and cooperative inhibition by glucose 1-phosphate in combination with trehalose 6-phosphate. *Plant Physiology and Biochemistry* 63: 89-98**

Pubmed: [Author and Title](#)

CrossRef: [Author and Title](#)

Google Scholar: [Author Only Title Only Author and Title](#)

**Paul MJ, Nuccio ML, Basu SS (2017) Are GM crops for yield and resilience possible? *Trends in Plant Science* doi.org/10.1016/j.tplants.2017.09.007**

**Pellny TK, Ghannoum O, Conroy JP, Schluempmann H, Smeekens S, Andralojc J, Krause K-P, Goddijn O, Paul MJ (2004) Genetic modification of photosynthesis with, *E. coli* genes for trehalose synthesis. *Plant Biotechnol J* 2: 71-82**

Pubmed: [Author and Title](#)

CrossRef: [Author and Title](#)

Google Scholar: [Author Only Title Only Author and Title](#)

**Ramon M, de Smet I, Vanesteene L, Naudts M, Leyman B, Van Dijck P, Rolland F, Beekman T, Thevelein JM (2009) Extensive expression regulation and lack of heterologous enzymatic activity of the Class II trehalose metabolism proteins from *Arabidopsis thaliana*. *Plant Cell and Environment* 32, 1015-1032**

Pubmed: [Author and Title](#)

CrossRef: [Author and Title](#)

Google Scholar: [Author Only Title Only Author and Title](#)

**Ray DK, Mueller ND, West PC, Foley JA (2013) Yield trends are insufficient to double global crop production by 2050. *PLoS ONE*. 8: e66428**

Pubmed: [Author and Title](#)

CrossRef: [Author and Title](#)

Google Scholar: [Author Only Title Only Author and Title](#)

**Risso D, Schwart K, Sherlock G, Dudoit S (2011) GC-Content Normalization for RNA-Seq Data. *BMC Bioinformatics* 12:480**

Pubmed: [Author and Title](#)

CrossRef: [Author and Title](#)

Google Scholar: [Author Only Title Only Author and Title](#)

**Robinson MD, McCarthy DJ, Smyth GK (2010) edgeR: A Bioconductor package for differential expression analysis of digital gene expression data. *Bioinformatics* 26, 139-140**

Pubmed: [Author and Title](#)

CrossRef: [Author and Title](#)

Google Scholar: [Author Only Title Only Author and Title](#)

**Romero C, Belles JM, Vaya JL, Serrano R, Culiñez-Macia FA (1997) Expression of the yeast trehalose-6-phosphate synthase gene in transgenic tobacco plants: pleiotropic phenotypes include drought tolerance. *Planta* 201: 293-297**

Pubmed: [Author and Title](#)

CrossRef: [Author and Title](#)

Google Scholar: [Author Only Title Only Author and Title](#)

**Ruiz-Salas, J-L, Ruiz-Medrano, R, Montes-Horcasitas, MC, Agreda-Laguna, KA, Hinojosa-Moya, J, Xoconostle-Cazares, B (2016) Vascular expression of trehalose phosphate synthase1 (TPS1) induces flowering in *Arabidopsis*. *Plant Omics* 9: 344-351**

Pubmed: [Author and Title](#)

CrossRef: [Author and Title](#)

Google Scholar: [Author Only Title Only Author and Title](#)

**Schluempmann H, Pellny T, van Dijken A, Smeekens S, Paul MJ (2003) Trehalose 6-phosphate is indispensable for carbohydrate utilisation and growth in *Arabidopsis thaliana*. *Proceedings of National Academy of Sciences* 100: 6849-6854**

Pubmed: [Author and Title](#)

CrossRef: [Author and Title](#)

Google Scholar: [Author Only Title Only Author and Title](#)

**Schluempmann H, van Dijken A, Aghdasi M, Wobbes B, Paul M, Smeekens S (2004) Trehalose-mediated growth inhibition of *Arabidopsis* seedlings is due to trehalose-6-phosphate accumulation. *Plant Physiology*: 135, 879-890**

Pubmed: [Author and Title](#)

CrossRef: [Author and Title](#)

Google Scholar: [Author Only Title Only Author and Title](#)

**Schussler JR, Westgate ME (1991a) Maize kernel set at low water potential: II. Sensitivity to reduced assimilates at pollination. *Crop Sci* 31: 1196-1203**

Pubmed: [Author and Title](#)

CrossRef: [Author and Title](#)

Google Scholar: [Author Only Title Only Author and Title](#)

**Schussler JR, Westgate ME (1991b) Maize kernel set at low water potential: I. sensitivity to reduced assimilates during early kernel growth. *Crop Sci* 31: 1189–1195**

Pubmed: [Author and Title](#)

CrossRef: [Author and Title](#)

Google Scholar: [Author Only](#) [Title Only](#) [Author and Title](#)

**Takagi H, Ishiga Y, Watanabe S, Konishi T, Egusa M, Akiyoshi N, Matsuura T, Mori IC, Hirayama T, Kaminaka H, Shimada H, Sakamoto A (2016) .Allantoin, a stress-related purine metabolite, can activate jasmonate signaling in a MYC2-regulated and abscisic acid-dependent manner. *J Exp Bot* 67: 2519-2532**

Pubmed: [Author and Title](#)

CrossRef: [Author and Title](#)

Google Scholar: [Author Only](#) [Title Only](#) [Author and Title](#)

**Trapnell C, Pachter, Salzberg SL (2009) TopHat: discovering splice junctions with RNA-Seq. *Bioinformatics* 25(9):1105-1111**

Pubmed: [Author and Title](#)

CrossRef: [Author and Title](#)

Google Scholar: [Author Only](#) [Title Only](#) [Author and Title](#)

**Tsai AY, Gazzarini S (2014) Trehalose-6-phosphate and SnRK1 kinases in plant development and signaling: the emerging picture. *Frontiers in Plant Science* 119: doi: 10.3389/fpls.2014.00119**

Pubmed: [Author and Title](#)

CrossRef: [Author and Title](#)

Google Scholar: [Author Only](#) [Title Only](#) [Author and Title](#)

**Virlouver L, Jacquemot M-P, Gernetes D, Corti H, Bouton S, Gilard F, Valot B, Trouverie J, Tcherkez G, Falque M, Damerval C, Rogowsky P, Perez P, Noctor G, Zivy M, Coursol S (2011) The ZmASR1 protein influences branched-chain amino acid biosynthesis and maintains kernel yield in maize under water-limited conditions. *Plant Physiology* 157, 917-936**

Pubmed: [Author and Title](#)

CrossRef: [Author and Title](#)

Google Scholar: [Author Only](#) [Title Only](#) [Author and Title](#)

**Wu D, Lim E, Vaillant F, Asselin-Labat ML, Visvader JE, Smyth GK (2010) ROAST: rotation gene set tests for complex microarray experiments. *Bioinformatics* 26, 2176–2182**

Pubmed: [Author and Title](#)

CrossRef: [Author and Title](#)

Google Scholar: [Author Only](#) [Title Only](#) [Author and Title](#)

**Yadav UP, Ivakov A, Feil R, Duan GY, Walther D, Giavalisco P, Piques M, Carillo P, Hubberten HM, Stitt M, Lunn JE (2014) The sucrose-trehalose 6-phosphate nexus: specificity and mechanisms of sucrose signalling by Tre6P. *J Exp Bot* 65: 1051-1068**

Pubmed: [Author and Title](#)

CrossRef: [Author and Title](#)

Google Scholar: [Author Only](#) [Title Only](#) [Author and Title](#)

**Zhang Y, Primavesi LF, Jhurrea D, Andralojc PJ, Mitchell RAC, Powers SJ, Schlupepmann H, Delatte T, Wngler A, Paul MJ (2009) Inhibition of Snf1-related protein kinase (SnRK1) activity and regulation of metabolic pathways by trehalose 6-phosphate. *Plant Physiology* 149: 1860-1871**

Pubmed: [Author and Title](#)

CrossRef: [Author and Title](#)

Google Scholar: [Author Only](#) [Title Only](#) [Author and Title](#)

**Zinselmeier C, Westgate ME, Schussler JR, Jones RJ (1995a) Low water potential disrupts carbohydrate metabolism in maize (*Zea mays* L.) ovaries. *Plant Physiol* 107: 385–391**

Pubmed: [Author and Title](#)

CrossRef: [Author and Title](#)

Google Scholar: [Author Only](#) [Title Only](#) [Author and Title](#)

**Zinselmeier C, Lauer MJ, Boyer JS (1995b) Reversing drought-induced losses in grain yield: sucrose maintains embryo growth in maize. *Crop Sci* 35: 1390–1400**

Pubmed: [Author and Title](#)

CrossRef: [Author and Title](#)

Google Scholar: [Author Only](#) [Title Only](#) [Author and Title](#)